AMERICAN SOCIETY FOR MICROBIOLOGY | Journal of Virology®

VIRUS-CELL INTERACTIONS

Co-opted Cellular Sac1 Lipid Phosphatase and PI(4)P Phosphoinositide Are Key Host Factors during the Biogenesis of the Tombusvirus Replication Compartment

Zsuzsanna Sasvari,[a] Wenwu Lin,[a] Jun-Ichi Inaba,[a] Kai Xu,[a] Nikolay Kovalev,[a] Peter D. Nagy[a]

[a]Department of Plant Pathology, University of Kentucky, Lexington, Kentucky, USA

Zsuzsanna Sasvari, Wenwu Lin, and Jun-Ichi Inaba contributed equally. The author order was determined based on the time of joining the project.

ABSTRACT Positive-strand RNA [(+)RNA] viruses assemble numerous membrane-bound viral replicase complexes (VRCs) with the help of viral replication proteins and co-opted host proteins within large viral replication compartments in the cytosol of infected cells. In this study, we found that deletion or depletion of Sac1 phosphatidylinositol 4-phosphate [PI(4)P] phosphatase reduced tomato bushy stunt virus (TBSV) replication in yeast (*Saccharomyces cerevisiae*) and plants. We demonstrate a critical role for Sac1 in TBSV replicase assembly in a cell-free replicase reconstitution assay. The effect of Sac1 seems to be direct, based on its interaction with the TBSV p33 replication protein, its copurification with the tombusvirus replicase, and its presence in the virus-induced membrane contact sites and within the TBSV replication compartment. The proviral functions of Sac1 include manipulation of lipid composition, sterol enrichment within the VRCs, and recruitment of additional host factors into VRCs. Depletion of Sac1 inhibited the recruitment of Rab5 GTPase-positive endosomes and enrichment of phosphatidylethanolamine in the viral replication compartment. We propose that Sac1 might be a component of the assembly hub for VRCs, likely in collaboration with the co-opted the syntaxin18-like Ufe1 SNARE protein within the TBSV replication compartments. This work also led to demonstration of the enrichment of PI(4)P phosphoinositide within the replication compartment. Reduction in the PI(4)P level due to chemical inhibition in plant protoplasts; depletion of two PI(4)P kinases, Stt4p and Pik1p; or sequestration of free PI(4)P via expression of a PI(4)P-binding protein in yeast strongly inhibited TBSV replication. Altogether, Sac1 and PI(4)P play important proviral roles during TBSV replication.

IMPORTANCE Replication of positive-strand RNA viruses depends on recruitment of host components into viral replication compartments or organelles. Using TBSV, we uncovered the critical roles of Sac1 PI(4)P phosphatase and its substrate, PI(4)P phosphoinositide, in promoting viral replication. Both Sac1 and PI(4)P are recruited to the site of viral replication to facilitate the assembly of the viral replicase complexes, which perform viral RNA replication. We found that Sac1 affects the recruitment of other host factors and enrichment of phosphatidylethanolamine and sterol lipids within the subverted host membranes to promote optimal viral replication. In summary, this work demonstrates the novel functions of Sac1 and PI(4)P in TBSV replication in the model host yeast and in plants.

KEYWORDS PI(4)P, lipid phosphatase, membrane contact site, membranes, plant, replication, sterol, tomato bushy stunt virus, virus-host interaction, yeast

Positive-strand RNA [(+)RNA] viruses assemble numerous membrane-bound viral replicase complexes (VRCs) within large viral replication compartments in the cytosol of infected cells (1–10). The viral replication proteins with co-opted host

Citation Sasvari Z, Lin W, Inaba J-I, Xu K, Kovalev N, Nagy PD. 2020. Co-opted cellular Sac1 lipid phosphatase and PI(4)P phosphoinositide are key host factors during the biogenesis of the tombusvirus replication compartment. J Virol 94:e01979-19. https://doi.org/10.1128/JVI.01979-19.

Editor Anne E. Simon, University of Maryland, College Park

Address correspondence to Peter D. Nagy, pdnagy2@uky.edu.

Received 22 November 2019
Accepted 2 April 2020
Accepted manuscript posted online 8 April 2020
Published 1 June 2020

proteins are involved in the biogenesis of replication compartments. In addition to membrane deformations and membrane proliferation, (+)RNA viruses also retarget cellular trafficking pathways and induce lipid biosynthesis to achieve robust replication (3, 6, 10–13). In spite of major recent advances in virus-host interactions, we still have not identified many of the subverted host factors in the biogenesis of VRCs and replication compartments, or their roles have not been defined.

Tomato bushy stunt virus (TBSV) and other tombusviruses code for two viral replication proteins, termed p33 and p92^{pol}, which are essential for virus replication (14–16). The TBSV p33 replication protein is the master regulator of VRC assembly and viral (+)RNA recruitment into VRCs. The auxiliary p33 has an RNA chaperone function. p92^{pol} is the viral RNA-dependent RNA polymerase (RdRp) that synthesizes the viral RNA progeny. The N-terminal segment of p92^{pol} is identical to p33 due to the translational readthrough of the stop codon in the p33 open reading frame (ORF). TBSV forms numerous VRCs, spherule-like structures that are vesicles with narrow openings toward the cytosol, utilizing peroxisomal membranes in plants and yeast (*Saccharomyces cerevisiae*), a model host (17–19).

Intensive research with TBSV in yeast has led to the identification of a long list of host factors co-opted for viral RNA replication (3, 5, 20, 21). Genomics- and lipidomics-based results also demonstrated a major role for global phospholipid and sterol biosynthesis in TBSV replication (22–24). Lipids, including phosphatidylethanolamine (PE), phosphatidylinositol 3-phosphate [PI(3)P] phosphoinositide, and sterols, play essential roles in the biogenesis of tombusviral replication compartments, the formation of VRCs, and activation of the virus-encoded p92 RdRp (25–30).

TBSV replication triggers characteristic alterations in cells, including stabilization of the actin network, recruitment of endosomal and COPII vesicles into the viral replication compartments, induction of subcellular membrane proliferation, aggregation of peroxisomes, and exploitation of the ATP-generating glycolytic and fermentation pathways (26, 30–36). Another feature of TBSV replication is the formation/stabilization of membrane contact sites (MCSs) between the endoplasmic reticulum (ER) and peroxisomes, which are required for sterol enrichment within the replication compartment to support efficient virus replication (5, 19, 37–39).

In this study, we dissected the proviral function of Sac1 (suppressor of actin mutations 1-like protein) lipid phosphatase, which was identified as a pro-TBSV host factor in an earlier high-throughput genome-wide screen in yeast (40). Sac1 is a phosphatidylinositol 4-phosphate [PI(4)P] lipid phosphatase that is conserved in eukaryotes (41–43). Sac1 controls several cellular processes, including phosphoinositide homeostasis, membrane trafficking, and actin dynamics (44, 45). The best-documented function of Sac1 is to facilitate the formation of MCSs, where nonvesicular lipid exchange could take place between various organelles (41–43, 46). The ER-resident Sac1 PI(4)P phosphatase is a critical cellular protein in MCS formation/function because it allows the directional transfer of sterols from the ER to the acceptor membranes by converting PI(4)P phosphoinositide to PI phosphatidylinositol. PI(4)P is needed by oxysterol binding proteins (OSBP in mammals, Osh proteins in yeast, and ORP proteins in plants) to exchange for sterols/oxysterols/ergosterols to transfer these lipids at the MCS (47–51). PI(4)P and Sac1 also affect phosphatidylserine transport at the MCS (52).

Sac1 is a transmembrane protein with both N- and C-terminal domains exposed to the cytosol. Deletion of *SAC1* in yeast and mammalian cells leads to changes in Golgi apparatus morphology and function, and *sac1* knockout in a mouse is embryonically lethal. It has been reported previously that Sac1 is localized to the Golgi membranes only when cells are starved for nutrients or growth factors but remains in the ER under normal growth conditions (45, 53, 54).

Mutations in Sac1 are involved in several human diseases, including the progression of breast cancer cells by regulating PI(4)P levels and the expression of CD44, a transmembrane receptor, which regulates cell adhesion and migration in breast cancer cells (45, 55–57).

There are nine Sac1 domain proteins in *Arabidopsis thaliana* (AtSac1 proteins), and

three of them, namely, Sac1a, Sac1b, and Sac1c, could complement the *sac1*-null (*sac1*Δ) mutant of yeast; these proteins are also localized to the ER and have PI(4)P phosphoinositide phosphatase activity (58–60).

Identification of the critical proviral function of Sac1 opens up the possibility that PI(4)P phosphoinositide might affect tombusvirus replication. PI(4)P, similar to other PI phosphoinositides, is a minor, yet essential, component of the cytosolic leaflet of certain eukaryotic cell membranes (53). In general, phosphorylation or dephosphorylation of PI phosphoinositides, which are guided by responses to acute signaling inputs, provides spatial and temporal cues within the cell for phosphoinositide-binding proteins. These, in turn, promote the assembly of macromolecular complexes and initiate several physiological events, including membrane trafficking and actin dynamics (53).

In this paper, we find that deletion or depletion of Sac1 affected TBSV replication in yeast and plant cells. We document reduction in the size of viral replication compartments in *sac1*Δ yeast. Moreover, the effect of Sac1 seems to be direct, based on interaction with the p33 replication protein, copurification with the tombusvirus replicase, and its presence in the TBSV replication compartment in yeast cells. Altogether, we demonstrate a critical role for Sac1 in TBSV replication and propose that the proviral functions of Sac1 might include manipulation of lipid composition within VRCs. In addition, Sac1 might serve as an assembly platform for VRCs within the extensive TBSV replication compartments in cells.

RESULTS

The cellular Sac1 lipid phosphatase is critical for tombusvirus replication in yeast and plants. To test the role of cellular Sac1p in tombusvirus replication, we launched TBSV replicon RNA (repRNA) replication in *sac1*Δ yeast from plasmids expressing the viral p33 and p92^{pol} replication proteins together with DI-72 repRNA. The TBSV repRNA, which contains four noncontiguous segments from the genomic RNA (gRNA), can replicate efficiently in yeast and plant cells expressing p33 and p92^{pol} (16, 61). Northern blot analysis revealed low-level TBSV repRNA replication (11 to 23% of that found in wild-type [WT] yeast) (Fig. 1A and B, compare lanes 4 to 6 to lanes 1 to 3). Western blot analysis showed that the tombusvirus p33 and p92^{pol} replication proteins were expressed at close to WT level (Fig. 1B). Plasmid-based expression of His_6-tagged Sac1p in *sac1*Δ yeast increased TBSV repRNA accumulation to ~170% (Fig. 1C, lanes 10 to 12), indicating that the defect in *sac1*Δ yeast can be complemented. Overexpression of Sac1p in WT yeast resulted in an ~3-fold increase in TBSV repRNA accumulation (Fig. 1C, lanes 7 to 9 versus lanes 1 to 3), suggesting that the amount of Sac1p available for TBSV replication is limited in WT yeast. Altogether, these data firmly established that cellular Sac1p is a critical proviral factor for TBSV replication in yeast.

To test the relevance of Sac1 in TBSV replication in a plant system, we focused on Sac1a/b/c, which were shown to have PI(4)P phosphatase activities and could complement *SAC1* deletion in yeast (59, 62). First, we used a virus-induced gene silencing (VIGS) approach to deplete the Sac1a level in *Nicotiana benthamiana*, which resulted in downregulation of Sac1a mRNA (Fig. 1D). Replication of the infectious TBSV gRNA was decreased by ~3-fold in the Sac1a knockdown plants compared to the control nonsilenced plants (Fig. 1D, lanes 1 to 8 versus lanes 9 to 16). Second, VIGS-based silencing of Sac1b also resulted in an ~3-fold reduction in TBSV replication in *N. benthamiana* (Fig. 1E). Altogether, these data suggest that cellular Sac1 is required for TBSV accumulation in plants. Thus, similar to the results obtained in yeast, the *SAC1* genes are major proviral factors in tombusvirus replication in plants.

Reduced *in vitro* replication of TBSV in the absence of Sac1. To obtain more direct evidence supporting the proviral role of Sac1p in TBSV replication, we prepared cell-free extracts (CFEs) from *sac1*Δ and WT yeasts, followed by *in vitro* reconstitution of the tombusvirus replicase using purified recombinant TBSV p33 and p92^{pol} replication proteins and T7-transcription-based repRNA template (63). CFEs from *sac1*Δ yeast supported ~90% less efficient *in vitro* replication of TBSV repRNA than CFEs prepared from WT yeast (Fig. 1F, compare lanes 5 and 6 with lanes 1 and 2).

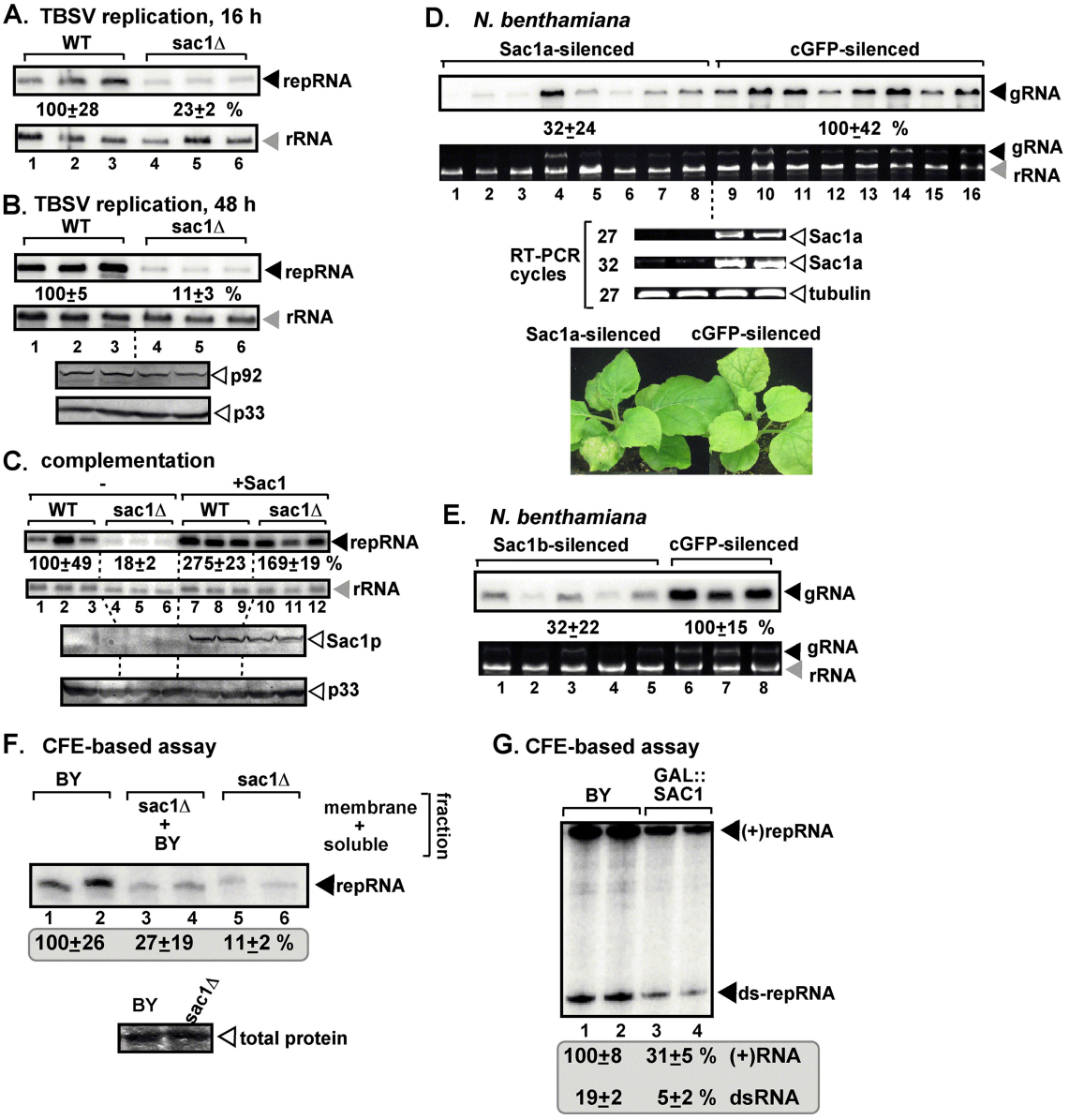

FIG 1 Sac1p PI(4)P phosphatase protein is an essential host factor for tombusvirus replication in yeast and plants. (A and B) Deletion of Sac1 inhibits TBSV replication in yeast. (Top gels) Northern blot analyses of TBSV repRNA using a 3′-end-specific probe demonstrate reduced accumulation of repRNA in the *sac1*Δ yeast strain (lanes 4 to 6) in comparison with the WT yeast strain (lanes 1 to 3). A plasmid-borne copper-inducible *CUP1* promoter was used to express the viral proteins His_6-p33 and His_6-p92, while DI-72 (+)repRNA was expressed from the constitutive *ADH1* promoter. Standard errors were calculated based on three separate repeats. TBSV repRNA accumulation was measured with a phosphorimager and normalized based on the 18S rRNA level. (Second gels) Northern blotting with 18S rRNA-specific probe was used as a loading control. (Bottom gels) Western blot analysis of the level of His_6-tagged proteins with anti-His antibodies. (C) Complementation of TBSV replication with His_6-Sac1 in the *sac1*Δ yeast strain. (Top gel) Northern blot analyses of repRNA using a 3′-end-specific probe. The viral proteins Flag-p33 and Flag-p92 were expressed from the *CUP1* promoter, whereas DI-72 (+)repRNA was expressed from the galactose-inducible *GAL1* promoter. (Second gel) Northern blot with 18S rRNA-specific probe used as a loading control. (Bottom gels) Western blot analysis of the levels of His_6-tagged Sac1 protein and Flag-p33 with anti-His and anti-Flag antibodies, respectively. Each experiment was repeated three times. (D and E) (Top gels) Accumulation of the TBSV gRNA in Sac1a-silenced or Sac1b-silenced *N. benthamiana* plants 2 days postinoculation (dpi) in the inoculated leaves was measured by Northern blot analysis. Inoculation of TBSV gRNA was done 8 days after starting VIGS. Agroinfiltration of the tobacco rattle virus (TRV) vector carrying NbSac1a, NbSac1b, or C-terminal GFP (as a control) sequence was used to induce VIGS. (Second gels) rRNA is shown as a loading control in an ethidium-bromide-stained agarose gel. (D) (Third gel) RT-PCR analysis of NbSac1a mRNA levels in the silenced and control plants. (Bottom) RT-PCR analysis of tubulin mRNA levels in the silenced and control plants. Each experiment was repeated three times. cGFP, C-terminal domain of GFP. (F) Reduced TBSV RNA replication by the reconstituted tombusvirus replicase in cell extracts (CFE) prepared from *sac1*Δ yeast in comparison to a similar CFE preparation obtained from WT yeast. Purified recombinant MBP-p33 and MBP-$p92^{pol}$ replication proteins of TBSV and *in vitro*-transcribed TBSV DI-72 (+)repRNA were added to the CFEs. The mixed CFE in lanes 3 and 4 contained the membrane fraction from *sac1*Δ CFE and the soluble fraction obtained from the WT (BY4741) yeast CFE. (G) Nondenaturing PAGE analysis showing the ^{32}P-labeled TBSV repRNA products, including the (+)repRNA progeny and the dsRNA replication intermediate, made by the reconstituted TBSV replicase. The CFEs used were from either WT yeast (BY4741) or Sac1-depleted GAL::SAC1 yeast strains (cultured in a raffinose medium).

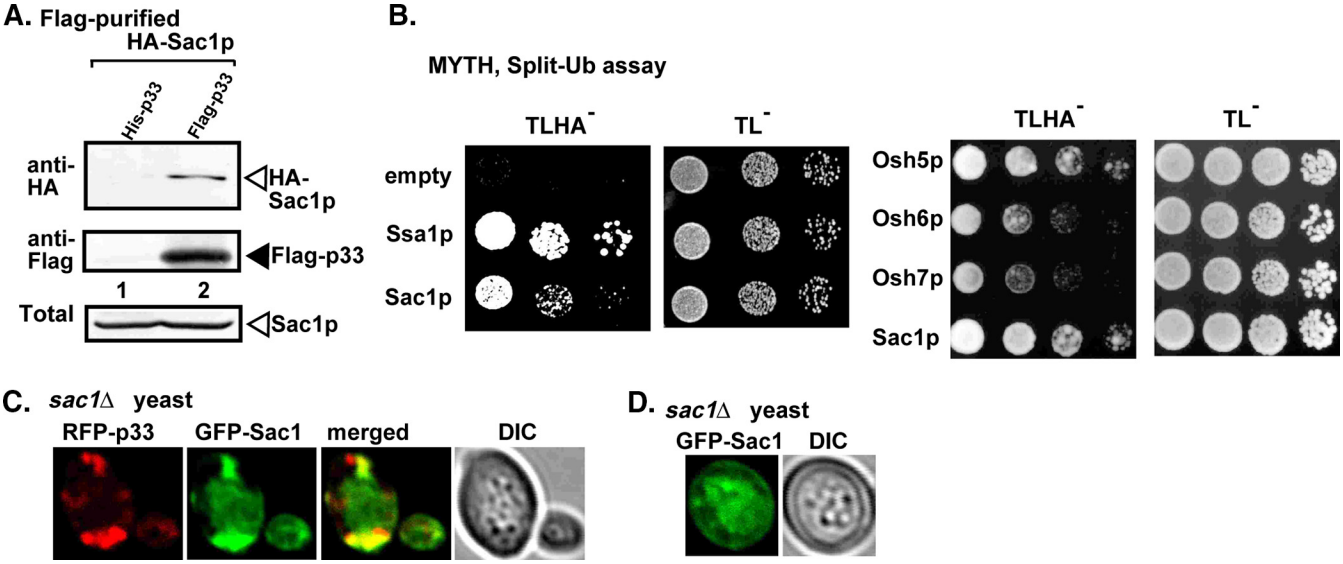

FIG 2 Interaction between tombusvirus replication proteins and Sac1. (A) Copurification of yeast 3×HA-Sac1 expressed under the natural promoter and from the original chromosomal location with TBSV Flag-p33 and Flag-p92^{pol} replication proteins from subcellular membranes. (Top two gels) Western blot analysis of copurified 3×HA-Sac1 (lanes 2) with Flag affinity-purified Flag-p33. HA-Sac1 and Flag-p33 were detected with anti-HA and anti-Flag antibodies, respectively. The negative control was from yeast expressing His$_6$-p33 and His$_6$-p92^{pol} purified in a Flag affinity column (lanes 1). (Bottom gel) Western blot of total 3×HA-Sac1 in the total yeast extracts. (B) The split ubiquitin (Ub)-based MYTH assay was used to test binding between TBSV p33 and the yeast Sac1 proteins in yeast. The bait p33 was coexpressed with the prey proteins shown. Ssa1p Hsp70 and the empty prey vector (NubG) were used as positive and negative controls, respectively. (Left) p33-Sac1 interactions. (Middle left) Demonstration that comparable amounts of yeasts were used for the experiments. (Middle right and right) Demonstration that the interaction of Sac1 with p33 is comparable to the interaction of the Osh proteins shown with p33. (C) Confocal microscopy images showing colocalization of TBSV RFP-p33 replication protein and GFP-Sac1 in *sac1*Δ yeast coexpressing p92^{pol} and repRNA. (D) Confocal microscopy images showing localization of GFP-Sac1 in *sac1*Δ yeast in the absence of TBSV components. DIC, differential inference contrast.

Since Sac1p is an ER-resident protein (45), we mixed the membrane fraction of CFEs from *sac1*Δ yeast with the soluble fraction from WT CFEs to assemble the replicase *in vitro*, followed by the replication assay. Interestingly, TBSV repRNA replication was supported at an ~4-fold-reduced level (Fig. 1F, lanes 3 and 4). Thus, the above-mentioned results demonstrate that the cellular Sac1p present in the membrane fraction of yeast is important for TBSV replication *in vitro*.

To test if either negative-strand synthesis or positive-strand synthesis of TBSV is inhibited when Sac1p is depleted, we used the CFE-based replicase reconstitution assay with purified recombinant p33 and p92^{pol} replication proteins and (+)repRNA template (63). The double-stranded RNA (dsRNA) replication intermediate product produced during minus-strand synthesis (64) was reduced by ~4-fold, whereas the (+)repRNA was decreased by ~3-fold in yeast with depleted Sac1p levels (Fig. 1G). Thus, depletion of Sac1p interfered with the synthesis of both RNA strands, which is likely the consequence of inhibition of the *in vitro* assembly of TBSV replicase.

The tombusvirus replication protein interacts with the ER-localized Sac1 protein. To explore if cellular Sac1p interacts with the TBSV p33 replication protein, we performed copurification experiments from yeast coexpressing Flag-tagged p33 and 3× hemagglutinin (3×HA)-tagged Sac1p. The yeast strain expressed 3×HA-tagged Sac1p under the native promoter from the original chromosomal location in the absence of WT Sac1p. After detergent solubilization of the membrane fraction and immobilization of Flag-p33 in the Flag-binding column, we eluted the bound proteins from the column, followed by Western blotting analysis. These assays revealed that Sac1p was copurified with p33 (Fig. 2A), suggesting that the proteins form a complex in yeast membranes. Similarly prepared yeast extract containing His$_6$-p33 excluded nonspecific binding by 3×HA-tagged Sac1p to the column. To further confirm the interaction, we conducted a split-ubiquitin-based membrane yeast two-hybrid (MYTH) assay (65). We found that p33 replication protein interacted with Sac1p in the MYTH assay (Fig. 2B), comparable to the interactions previously demonstrated between p33

and a select group of the yeast Osh proteins (oxysterol binding protein 1-like OSBP1/ORP proteins) (39).

To examine if the cellular Sac1p and the tombusvirus p33 replication protein are colocalized in yeast, we coexpressed the red fluorescent protein (RFP)-tagged p33 and the green fluorescent protein (GFP)-Sac1p in *sac1*Δ yeast cells. Confocal laser microscopy showed the colocalization of a fraction of RFP-p33 with a portion of GFP-Sac1 (Fig. 2C). The presence of Sac1p in large punctate structures formed during p33 expression in yeast (32) indicates that a fraction of Sac1p molecules are recruited into the tombusvirus replication compartment. In contrast, separate expression of GFP-Sac1p showed the characteristic ER distribution of Sac1p, which was not present in large punctate structures in the absence of the tombusvirus replication protein (Fig. 2D).

To extend our findings to plants, we expressed blue fluorescent protein (BFP)-tagged TBSV p33 replication protein and RFP-tagged *Arabidopsis* Sac1 by agroinfiltration in *N. benthamiana* leaves and followed their localization with confocal microscopy. The formation of p33-BFP-decorated replication compartments, with or without TBSV infection, showed the efficient colocalization of AtSac1 within the large TBSV replication compartments consisting of the aggregated peroxisomes, which were marked with GFP-SKL (Fig. 3A). In the absence of viral components, AtSac1 did not colocalize with the peroxisomal or nuclear markers (RFP-H2B) (Fig. 3A) or with the mitochondria (Fig. 4A).

To show that the recruitment of AtSac1 takes place in the active TBSV replication compartment, we monitored the accumulation of the replicating (+)repRNA with a biosensor detecting the newly generated (+)repRNA based on the incorporation of the MS2 bacteriophage RNA sequence, which is specifically recognized by the RFP-tagged MS2 coat protein (Fig. 3B) (66). These experiments confirmed the colocalization of co-opted AtSac1 with the replication compartment decorated with p33-BFP in *N. benthamiana*. Therefore, Sac1 likely plays a role in the formation of the tombusvirus replication compartments.

To provide additional evidence that the plant AtSac1 interacts with the TBSV p33 replication protein, we conducted bimolecular fluorescence complementation (BiFC) experiments with p33 and AtSac1 in *N. benthamiana* leaves. The BiFC signals revealed specific interactions between AtSac1 and p33 replication protein at the aggregated peroxisomes (Fig. 3C). Based on these data, we suggest that the cellular Sac1 lipid phosphatase is actively recruited into the large replication compartment induced by tombusviruses.

Similar confocal-microscopy-based experiments with the closely related carnation Italian ringspot virus (CIRV), which, unlike TBSV, builds replication compartments from aggregated mitochondria (67, 68), revealed the colocalization of AtSac1 with the CIRV p36-RFP replication protein and the GFP-AtTim21 mitochondrial membrane protein (Fig. 4A). We also conducted BiFC experiments, which revealed specific interactions between AtSac1 and the CIRV p36 replication protein at the aggregated mitochondria (Fig. 4B). Taken together, these data suggest that AtSac1 is recruited into the large mitochondrion-based CIRV replication compartment in plant cells.

Sac1 protein is recruited into tombusvirus-induced membrane contact sites. One of the known cellular functions of the ER-resident Sac1p is performed at MCSs between the ER and the plasma membrane (PM) or Golgi membrane, which are needed to transport sterols to the PM and PI(4)P to the ER as a counterflow. By converting PI(4)P to PI in the ER, Sac1p makes the lipid flow directional (42, 43). TBSV p33 replication protein has been shown to stabilize MCSs, termed vMCSs, between the ER and peroxisomes through interacting with the ER-resident Scs2p VAP protein and the OSBP1-like ORP proteins, such as Osh3p, -5, -6, and -7 (37, 40). To test the subcellular location of Sac1p in yeast replicating TBSV and if Sac1p is also recruited to vMCSs, we performed confocal-microscopy-based colocalization and BiFC experiments between p33 and Scs2p VAP tethering protein (69) in yeast. These studies indicated that Sac1p is recruited to the subcellular sites of p33-Scs2p interaction (Fig. 5A), which has been

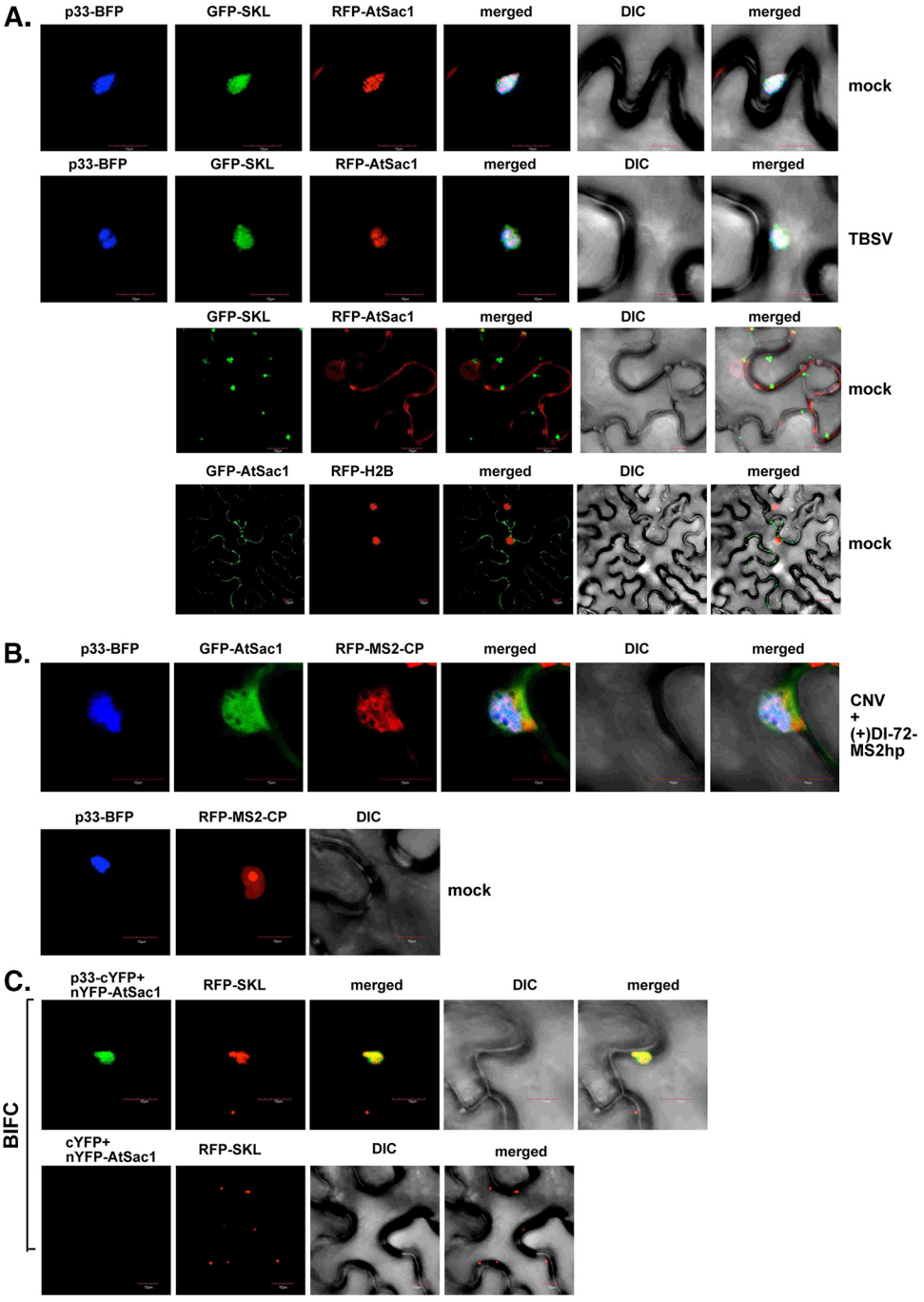

FIG 3 Recruitment of Sac1 by the TBSV p33 replication protein into the viral replication compartment in *N. benthamiana*. (A) (Top two rows) Confocal microscopy images showing efficient colocalization of TBSV p33-BFP replication protein and RFP-AtSac1 within the viral replication compartment marked by GFP-SKL peroxisomal marker in *N. benthamiana* leaves. Expression of these proteins from the 35S promoter was done after coagroinfiltration into *N. benthamiana* leaves. The plant leaves were either mock inoculated or TBSV infected, as shown. Scale bars, 10 μm. (Bottom two rows) Confocal microscopy images showing different localization patterns for AtSac1 in comparison with GFP-SKL peroxisomal marker or RFP-H2B nuclear marker in *N. benthamiana* leaves. (B) (Top row) GFP-AtSac1 is recruited into the replication compartment, which supports viral RNA synthesis. The viral (+)repRNA carried six copies of the RNA hairpin (MS2hp) from the MS2 bacteriophage, which is specifically recognized by the MS2 coat protein (RFP-MS2-CP). The replication compartment was marked by the BFP-tagged p33 replication protein in *N. benthamiana*. (Bottom row) Images of mock-inoculated plants (no viral RNA replication). Note that RFP-MS2-CP contains a weak nuclear localization signal; therefore, it is present in the nucleus in the absence of replicating (+)repRNA-MS2hp in the cytosol. Expression of the above-mentioned proteins from the 35S promoter was done after coagroinfiltration into *N. benthamiana* leaves. The images were taken 3.5 days after agroinfiltration of plant leaves. Scale bars. 10 μm. Each experiment was repeated three times. (C) (Top row) Interactions between TBSV p33-cYFP replication protein and the nYFP-AtSac1 protein were detected by BiFC. The

(Continued on next page)

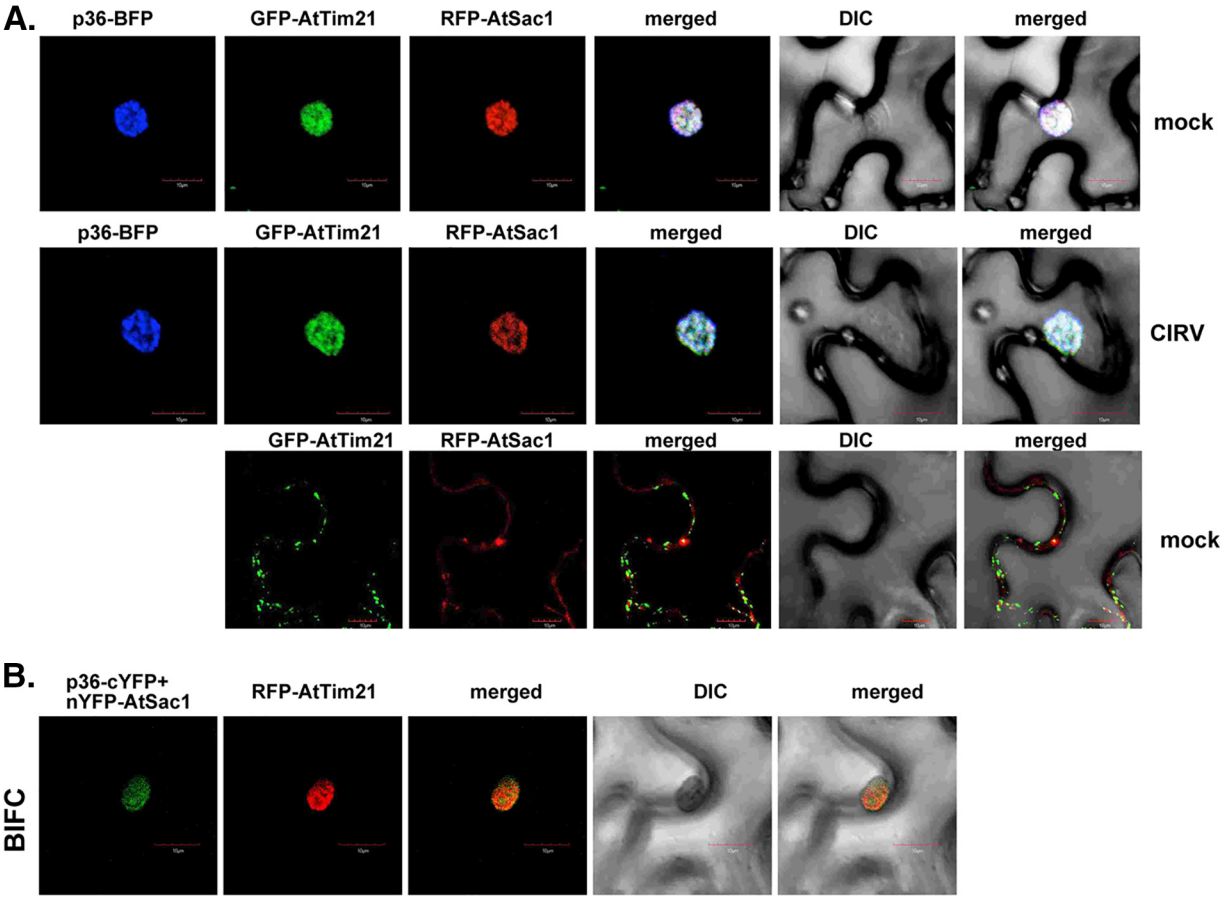

FIG 4 Recruitment of Sac1 by the CIRV p36 replication protein into the mitochondrion-derived viral replication compartment in *N. benthamiana*. (A) Confocal microscopy images showing efficient colocalization of CIRV p36-BFP replication protein and RFP-AtSac1 within the viral replication compartment, marked by the GFP-AtTim21 mitochondrial marker in *N. benthamiana* leaves. Further details are shown in Fig. 3A. (B) Interaction between CIRV p36-cYFP replication protein and the nYFP-AtSac1 protein was detected by BiFC. The merged images show efficient colocalization of RFP-AtTim21 with the BiFC signal, indicating that the interaction between the CIRV p36 replication protein and AtSac1 occurs at the aggregated mitochondria.

shown to take place in dedicated subdomains in the ER membranes, as part of vMCSs (39).

The vMCS-assisted enrichment of sterols at the replication sites is critical for TBSV replication (39). Accordingly, we colocalized RFP-p33, GFP-Sac1p, and ergosterol (stained with filipin) in yeast cells (Fig. 5B). The distribution of ergosterol changed in *sac1*Δ yeast, showing uneven, small, punctate-like structures, in contrast to the WT yeast, which showed the characteristic, mostly plasma membrane enrichment of ergosterol (Fig. 5C). Interestingly, the expression of the viral components in *sac1*Δ yeast also showed the uneven, punctate-like distribution of ergosterol, similar to the distribution in *sac1*Δ yeast not expressing viral components (Fig. 5C). As we demonstrated previously (39), the distribution of ergosterol is very different in WT yeast cells replicating TBSV RNA, showing large intracellular ergosterol-enriched punctate structures (Fig. 5C). Based on these data, we suggest that ergosterols are not efficiently redistributed to the sites of viral replication in *sac1*Δ yeast. Altogether, our data suggest that Sac1p is recruited into the tombusvirus replication compartment, including into vMCSs, to facilitate the redistribution of sterols to the sites of viral replication.

FIG 3 Legend (Continued)
merged image shows the efficient colocalization of RFP-SKL with the BiFC signal, indicating that the interaction between the p33 replication protein and AtSac1 takes place at the aggregated peroxisomes. (Bottom row) Negative control for the BiFC experiment.

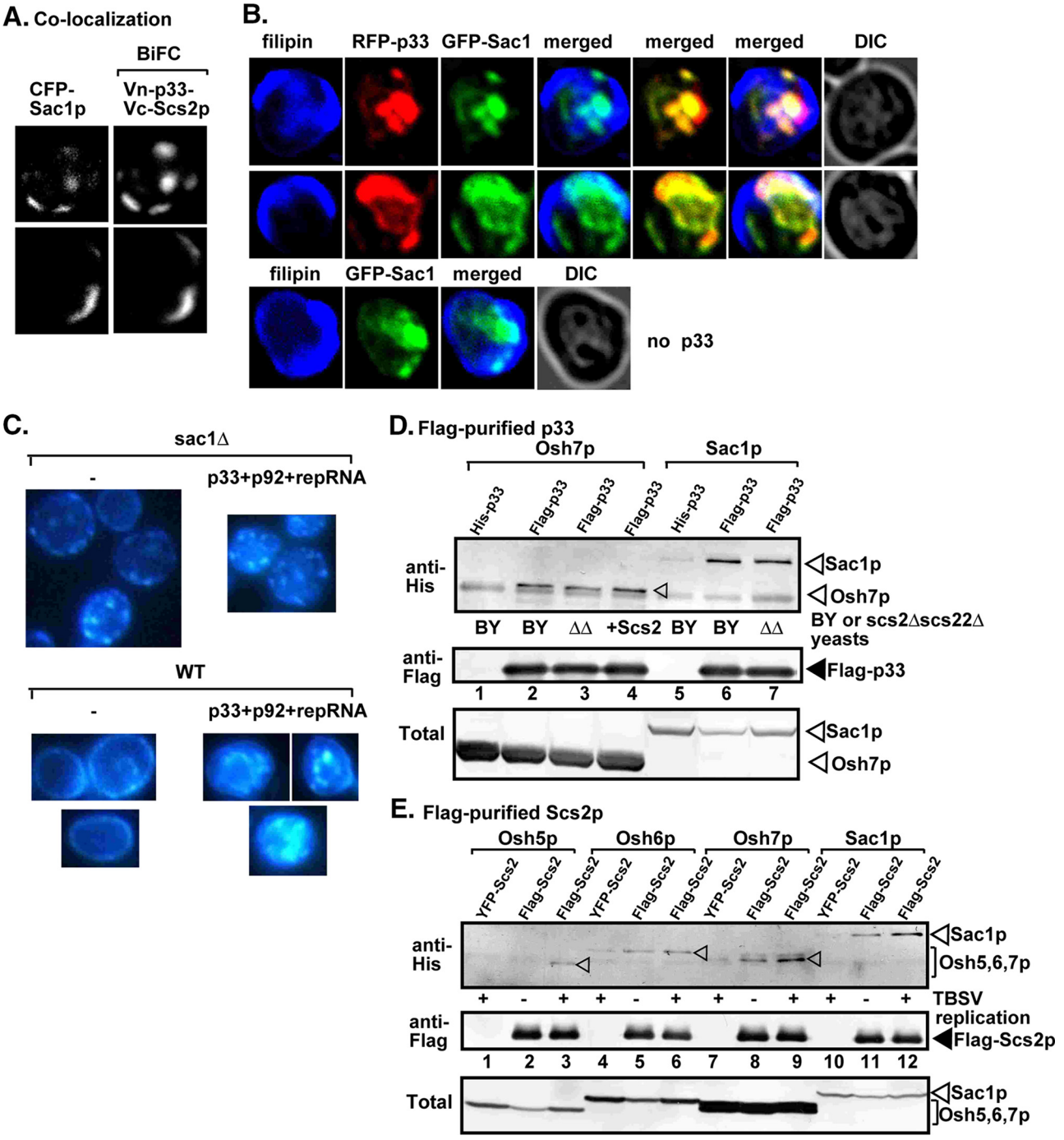

FIG 5 Effect of vMCS proteins on recruitment of Sac1 by the tombusvirus p33 replication protein in yeast. (A) Confocal microscopy images showing localization of yeast CFP-tagged Sac1p to vMCS marked by interaction between the p33 replication protein and the yeast Scs2p VAP protein, which was detected by BiFC. (B) Partial colocalization of ergosterols, RFP-p33, and GFP-Sac1 shown by confocal laser microscopy. Yeasts were stained with filipin dye to detect ergosterols. $p92^{pol}$ and the repRNA were not expressed in these yeast cells. (C) *SAC1* deletion prevents the formation of large sterol-enriched compartments in yeast replicating TBSV repRNA. Note the similar distributions of ergosterol in *sac1*Δ yeast with or without TBSV replication. Yeasts were stained with filipin dye to detect ergosterols. (D) Copurification of Sac1p and Osh7p proteins with the tombusvirus p33 replication protein from double-VAP-deletion (*scs2*Δ *scs22*Δ) (ΔΔ) yeast versus WT yeast. The Flag-tagged p33 was purified from the membrane fractions of yeast extracts using a Flag affinity column. Note that yeast coexpressed $p92^{pol}$ to support the replication of repRNA. (Top gel) Western blot analysis of copurified His_6-tagged Sac1p or His_6-Osh7 using anti-His antibody. The lane 4 sample was from WT yeast overexpressing Scs2p from a plasmid. (Middle gel) Western blot of purified Flag-p33 replication protein detected with anti-Flag antibody. (Bottom gel) Western blot of His_6-tagged Sac1p or His_6-Osh7 in the total yeast extracts using anti-His antibody. (E) Copurification of Sac1p and Osh5, -6, and -7 proteins with the Scs2 VAP protein from WT yeast replicating TBSV repRNA (coexpression of p33, p92, and repRNA; marked with "+") or without viral components (marked with "−").Flag-tagged Scs2p was purified from the membrane fractions of yeast extracts using a Flag affinity column. (Top gel) Western blot analysis of copurified His_6-Osh5, His_6-Osh6, His_6-Osh7, or His_6-Sac1 using anti-His antibody. (Middle gel) Western blot of purified Flag-Scs2p detected with anti-Flag antibody. (Bottom gel) Western blot of His_6-Osh5, His_6-Osh6, His_6-Osh7, or His_6-Sac1 in total yeast extracts using anti-His antibody.

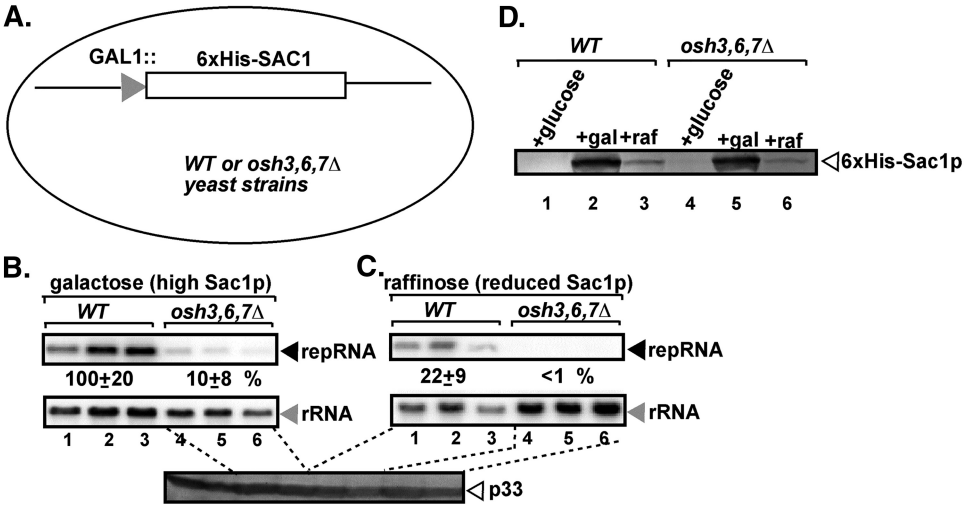

FIG 6 Sac1p PI(4)P phosphatase and the oxysterol binding proteins do not have complementary functions in tombusvirus replication in yeast. (A) Scheme of the expression strategy for Sac1p in WT yeast versus triple-deletion (*osh3,6,7*Δ) yeast. The His_6-Sac1p was expressed using the galactose-inducible *GAL1* promoter from its original chromosomal location in these haploid yeast strains. (B and C) Depletion of Sac1 inhibits TBSV replication in both WT and triple-deletion (*osh3,6,7*Δ) yeast strains. (Top gels) Northern blot analyses of repRNA using a 3′-end-specific probe demonstrating reduced accumulation of repRNA in either Sac1-induced (B) or Sac1-depleted (C) triple-deletion (*osh3,6,7*Δ) yeast strains. A plasmid-borne copper-inducible *CUP1* promoter was used to express the viral proteins His_6-p33 and His_6-p92, while DI-72 (+)repRNA was expressed from the constitutive *ADH1* promoter. (C) Note that we loaded twice as much RNA in lanes 4 to 6 than in lanes 1 to 3 to help visualize small amounts of repRNA. (Middle gels) Northern blotting with an 18S rRNA-specific probe was used as a loading control. (Bottom gel) Western blot analysis of the level of His_6-tagged p33 replication protein with anti-His antibodies. We loaded the same amount of total protein in each sample. (D) Western blot analysis of the levels of His_6-Sac1p in the indicated yeast strains cultured under repressive (glucose), inducing (galactose), or noninducing (raffinose) conditions.

To test if recruitment of Sac1p to the replication compartment is affected by the ER-resident Scs2p VAP tethering protein (and its paralog, Scs22p) (69), which is required for vMCS formation (39), we purified the tombusvirus replicase from *scs2*Δ *scs22*Δ yeast, followed by measuring the copurified His_6-Sac1p by Western blotting. In comparison with the replicase preparation from WT yeast, the replicase preparation from *scs2*Δ *scs22*Δ yeast contained a comparable amount of Sac1p (Fig. 5D, compare lanes 6 and 7), suggesting that the recruitment of Sac1p to the viral replication compartment is not dependent on the Scs2p/Scs22p VAP proteins. Similarly, the amount of Osh7p ORP in the replication compartment is only slightly affected by deletion of Scs2p/Scs22p VAP genes or overexpression of Scs2p in WT yeast (Fig. 5D, compare lanes 2, 3, and 4). These data suggest that p33 replication protein might recruit Sac1p and Osh7p cellular factors independently of Scs2p/Scs22p VAP proteins to the viral replication compartment in yeast.

To examine if the amounts of the co-opted cellular protein components of the virus-induced vMCSs are increased by p33/p92 replication proteins, we purified Flag-Scs2p VAP protein from detergent-solubilized membrane fractions of yeast replicating TBSV repRNA or missing the viral components as a control. As expected based on prior work (43, 69), His_6-Osh6p, His_6-Osh7p, and His_6-Sac1p were copurified with Flag-Scs2p from yeast lacking viral components (Fig. 5E). Interestingly, the amounts of His_6-Osh5p, His_6-Osh6p, His_6-Osh7p, and His_6-Sac1p copurified with Flag-Scs2p were increased in the presence of viral components (Fig. 5E). These data suggest that the expressed p33/p92 replication proteins stabilize the complexes containing the cellular Scs2p VAP, ORP proteins, and Sac1p, likely within vMCSs.

Testing TBSV replication in *osh3*Δ, *-6*Δ, and *-7*Δ yeast with depleted Sac1p showed undetectable TBSV repRNA accumulation levels (Fig. 6A to C), suggesting that both the ORP and Sac1p proteins are critical for TBSV replication in yeast. The additional inhibitory effect of Sac1p depletion on TBSV repRNA accumulation in *osh3*Δ, *-6*Δ, and

-*7*Δ yeast (Fig. 6C) in comparison with *osh3*Δ, -*6*Δ, and -*7*Δ yeast expressing high levels of Sac1p (Fig. 6B) indicates that Sac1p likely has other proviral functions in addition to its roles in vMCS and sterol enrichment (see below).

PI(4)P phosphoinositide is required for tombusvirus replication. Identification of the critical proviral function of Sac1p, which is a PI(4)P phosphatase (70), opens up the possibility that PI(4)P phosphoinositide might also affect tombusvirus replication. Therefore, we tested if depletion of PI(4)P kinases, which generate PI(4)P from PI, affects TBSV replication in yeast. Separate depletion of Stt4p and Pik1p PI(4)P kinases inhibited TBSV replication by ~4-fold (Fig. 7A and B), whereas deletion of the *LSB6* PI(4)P kinase gene in yeast had no effect (Fig. 7C). These data indicate that Stt4p and Pik1p PI(4)P kinases, which account for the vast majority of PI4 kinase (PI4K) activity in yeast cells (71), are critical host factors in TBSV replication, likely by providing PI(4)P.

To confirm the role of PI(4)P in plants, we used phenylarsine oxide (PAO), a specific inhibitor of PI(4)P kinases (72, 73) in *N. benthamiana* protoplasts replicating TBSV gRNA. PAO treatment resulted in undetectable accumulation of TBSV RNAs in plant cells (Fig. 7D), suggesting that PI(4)P is also critically important for tombusviruses in plant cells.

To test if PI(4)P is localized within the tombusvirus replication compartment, we coexpressed the GFP-tagged FAPP-PH domain, which specifically binds to PI(4)P (11, 74) in yeast. The yeast cells also coexpressed RFP-p33 and $p92^{pol}$ replication proteins and the TBSV repRNA to support the formation of the viral replication compartment and TBSV replication. Confocal microscopy revealed that GFP-FAPP-PH was partially colocalized with the RFP-p33 replication protein in yeast cells (Fig. 8A), indicating that PI(4)P was present within the viral replication compartment. The partial colocalization of p33 replication protein and PI(4)P phosphoinositide in yeast cells might be affected by the efficient utilization of PI(4)P by Sac1 at vMCSs, leading to reduction in PI(4)P levels and sterol enrichment within the viral replication compartment.

To further test the localization pattern of PI(4)P during virus replication, we expressed the DrrA effector protein of *Legionella pneumophila*, which through its C-terminal P4M domain binds exceptionally strongly to PI(4)P (75), thus possibly sequestering this minor lipid species away from the viral replication compartment inside the yeast cells. Expression of the DrrA effector changed the localization pattern of GFP-FAPP-PH (Fig. 8B). Moreover, RFP-p33 replication protein did not colocalize with GFP-FAPP-PH (Fig. 8B), suggesting that TBSV failed to recruit or enrich PI(4)P at the site of replication in the presence of the DrrA effector. We also noticed that DrrA expression inhibited the formation of the characteristic large replication compartments visible in WT yeast cells (compare Fig. 8A and B).

Using a similar approach in *N. benthamiana* plants through expression of GFP-FAPP-PH, we showed that PI(4)P accumulated within the large viral replication compartment detected via expression of p33-RFP in epidermal cells infected with TBSV (Fig. 8C). Expression of the DrrA effector in *N. benthamiana* leaves dramatically changed PI(4)P distribution and interfered with the formation of large replication compartments (Fig. 8D). Similar observations were made in *N. benthamiana* protoplasts replicating TBSV with PI(4)P-specific antibody. They included partial colocalization (enrichment) of PI(4)P with the p33 replication protein (Fig. 8E) and the absence of colocalization of PI(4)P with p33 when protoplasts were also coexpressing the DrrA effector (Fig. 8G). As expected based on the known localization pattern for PI(4)P, which includes the Golgi apparatus and the plasma membrane in plant cells (58, 60), PI(4)P was not colocalized with the peroxisomal marker in mock-transfected *N. benthamiana* protoplasts (Fig. 8F). Based on the above-mentioned data, we suggest that PI(4)P has a proviral function in tombusvirus replication and the DrrA effector, due to its strong binding to PI(4)P, sequesters PI(4)P, thus interfering with the enrichment of PI(4)P at the sites of tombusvirus replication.

Sac1 protein affects the recruitment of syntaxin18-like Ufe1p SNARE for tombusvirus replication. The formation of the TBSV replication compartment is a complex process depending on the ER-resident SNARE proteins, including the syntaxin18-like

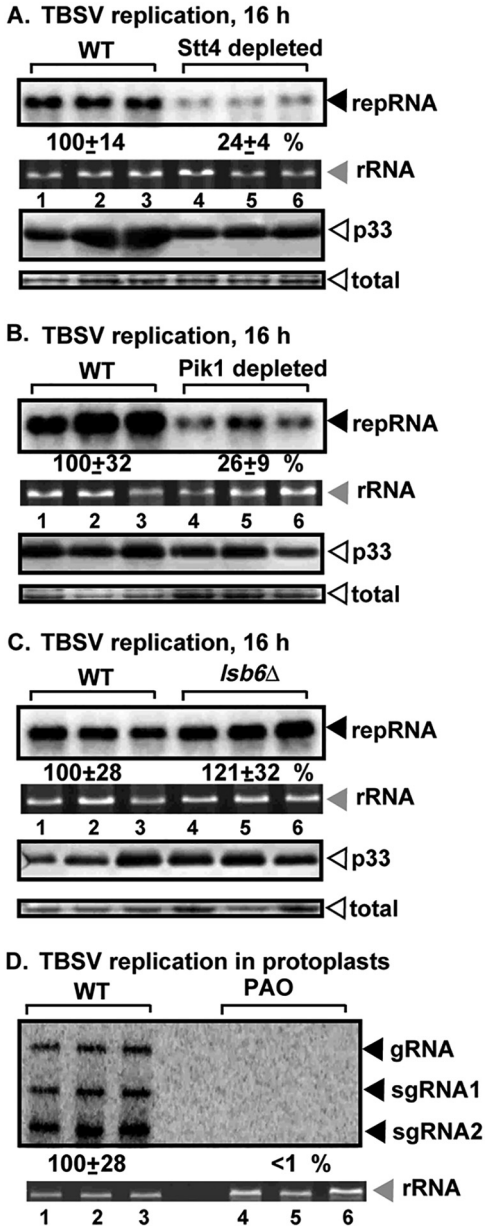

FIG 7 Depletion of PI4K enzymes reduces tombusvirus replication in yeast. (A and B) Depletion of Stt4p levels in TET::STT4 and Pik1p in TET::PIK1 yeast strains inhibits TBSV replication in yeast. Doxycycline (Dox) was used to downregulate the expression of Stt4p and Pik1p from the TET promoter. Replication of the TBSV repRNA in TET::STT4 and TET::PIK1 yeast strains, respectively, coexpressing the tombusvirus p33 and p92 replication proteins was measured by Northern blotting 16 h after initiation of TBSV replication. The accumulation level of His_6-p33 replication protein was tested by Western blotting and anti-His antibody. (C) Deletion of LSB6 PI4K does not inhibit TBSV replication in yeast. Northern and Western blot analyses were performed as for panel A. (D) Inhibition of PI4K enzymes by PAO decreases TBSV replication in *N. benthamiana* protoplasts. Three-week-old *N. benthamiana* leaves were used for protoplast preparations, which were transfected with TBSV RNAs using PEG4000. Incubation of protoplasts with PAO (50 μM) was for 16 h. Each experiment was repeated three times.

Ufe1p (38, 76). We have previously shown that depletion of Ufe1p inhibits the formation of tombusvirus replication compartments via multiple mechanisms (38). To study if recruitment of the ER-resident Ufe1p into the viral replication sites was affected by Sac1p, we examined the subcellular distribution of RFP-Ufe1p in *sac1*Δ yeast via confocal microscopy. We observed that Ufe1p colocalized poorly with p33 replication protein within the small p33-containing punctate structures formed in *sac1*Δ yeast in

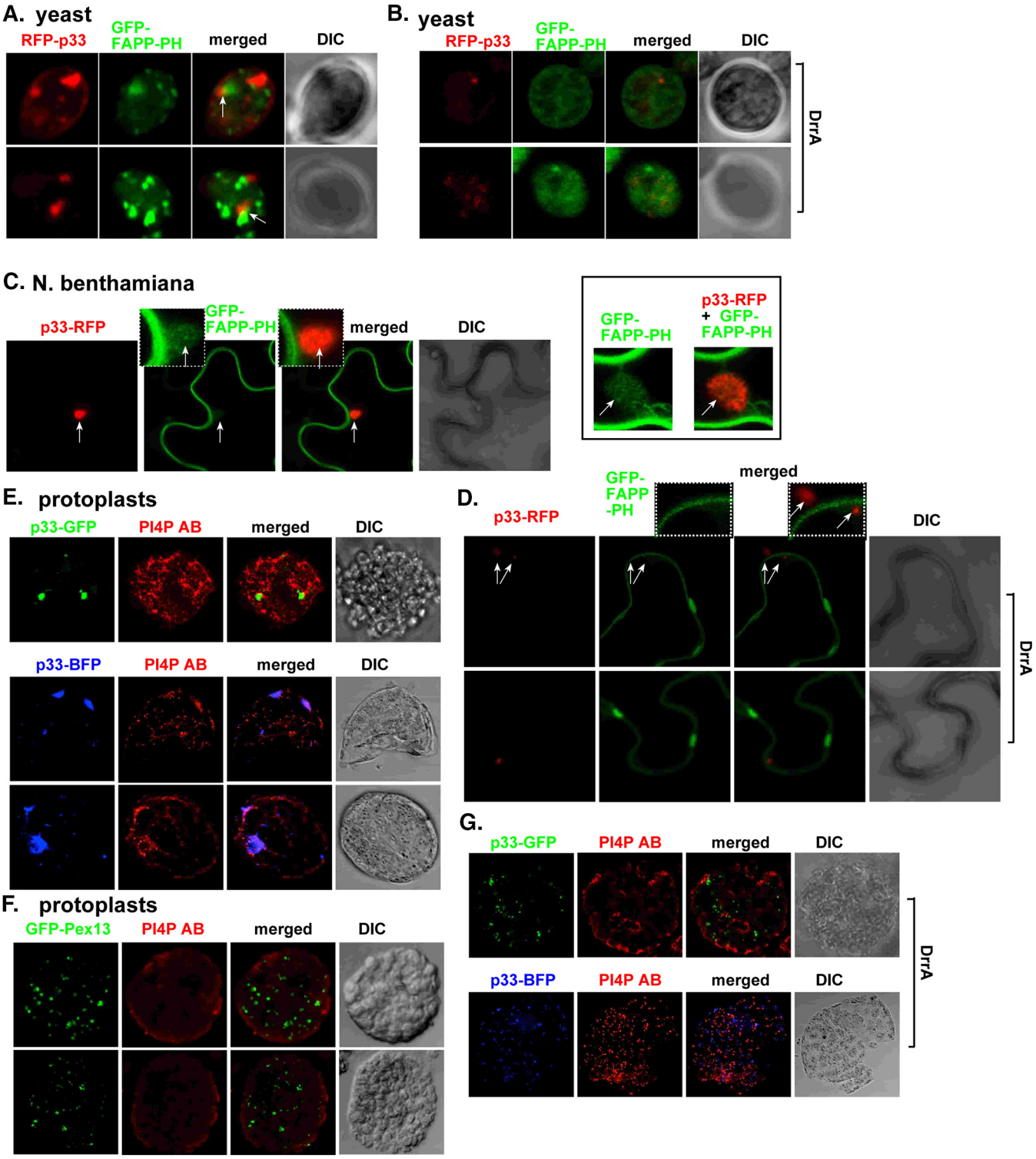

FIG 8 Partial colocalization of PI(4)P phosphoinositide with the TBSV p33 replication protein in yeast and in *N. benthamiana*. (A) Confocal microscopy images showing partial colocalization of TBSV RFP-p33 with GFP-FAPP-PH, which specifically binds to PI(4)P in yeast. The arrows point to the areas where colocalization was detected. The yeast also coexpressed $p92^{pol}$ and repRNA to support TBSV replication. (B) Expression of the *Legionella* DrrA effector, which binds strongly to PI(4)P through its C-terminal P4M domain, eliminates colocalization of TBSV RFP-p33 with GFP-FAPP-PH in yeast cells. Note that the p33 replication protein cannot form the large replication compartment in these cells. Further details are shown in panel A. (C) Confocal microscopy images showing partial colocalization of TBSV p33-RFP with GFP-FAPP-PH in *N. benthamiana*. The arrows point to the areas where colocalization was detected. The boxed images on the right are different from those on the left. Expression of these proteins from the 35S promoter was done after coagroinfiltration into *N. benthamiana* leaves replicating TBSV. (D) Expression of the *Legionella* DrrA effector interferes with the colocalization of TBSV p33-RFP with GFP-FAPP-PH in *N. benthamiana* cells. Note that p33 replication protein cannot form the large replication compartment in these cells. Further details are shown in panel C. (E) Confocal microscopy images showing partial colocalization of either p33-GFP or p33-BFP and PI(4)P in *N. benthamiana* protoplasts. *N. benthamiana* plants were agroinfiltrated to

(Continued on next page)

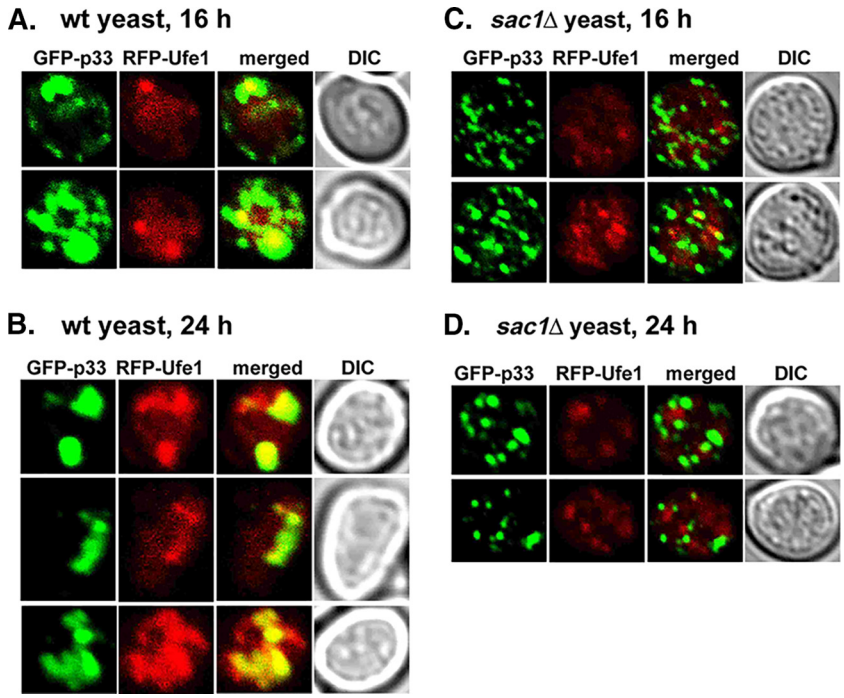

FIG 9 Recruitment of the syntaxin18-like Ufe1 SNARE by the TBSV p33 replication protein is inhibited in *sac1*Δ yeast. (A and B) Confocal microscopy images showing the colocalization of GFP-p33 with RFP-Ufe1 in WT yeast at 16 and 24 h of incubation. (C and D) Confocal microscopy images showing lack of colocalization of GFP-p33 with RFP-Ufe1 in *sac1*Δ yeast at 16 and 24 h of incubation. Note that the yeast cells did not express $p92^{pol}$ and repRNA. Each experiment was repeated three times.

contrast with the more extensive colocalization between Ufe1p and p33 in WT yeast at two different time points (Fig. 9C and D versus Fig. 9A and B).

To test if Sac1p affects the recruitment of Ufe1p to the vMCSs, we visualized vMCSs via BiFC using VN-p33 and VC-Scs2 VAP protein (39). We found that Ufe1p was poorly colocalized with p33-Scs2p-decorated membranes in *sac1*Δ yeast in contrast with the more extensive colocalization in WT yeast (Fig. 10B versus Fig. 10A). These data support a model in which Sac1p is critical for the efficient recruitment of Ufe1p SNARE protein into the p33-containing replication compartment and to the vMCS.

Sac1p is required for the efficient recruitment of p33-driven Rab5-positive endosomes into the replication compartment in yeast. The biogenesis of the large TBSV replication compartments, which consist of the Scs2p VAP-containing vMCSs and the Ufe1p-containing ER arrival site (ERAS) subdomains of the ER and numerous VRCs within aggregated peroxisomes, depends on retargeting of Rab5-positive endosomes, which are PE rich, to the sites of viral replication (19, 26, 30). To test if Sac1p affects the recruitment of Rab5-positive endosomes, we used confocal microscopy in combination with BiFC analysis. These experiments showed that the Rab5 (called Vps21 in yeast)-positive endosomes were not colocalized with the p33 replication protein-Scs2p VAP complex in *sac1*Δ yeast (Fig. 11B), whereas we observed partial colocalization in WT yeast (Fig. 11A).

FIG 8 Legend (Continued)
express either p33-GFP or p33-BFP. The next day, *N. benthamiana* protoplasts were prepared from the agroinfiltrated plants and transfected with TBSV gRNA. After 16 h of incubation, the protoplasts were fixed. Note that PI(4)P was detected by PI(4)P-specific antibody after the permeabilization of protoplasts. (F) Lack of colocalization of peroxisomes, marked by GFP-Pex13 and PI(4)P in *N. benthamiana* protoplasts lacking viral components. Note that PI(4)P was detected by PI(4)P-specific antibody. (G) Expression of the *Legionella* DrrA effector prevents the colocalization of TBSV p33-RFP or p33-BFP with PI(4)P in *N. benthamiana* protoplasts. Agroinfiltration was used to express DrrA, p33-GFP, and p19 suppressor of gene silencing for 1 day in *N. benthamiana* leaves, followed by protoplast isolation. Then, the protoplast preparations were transfected with TBSV RNA, followed by incubation for 16 h. PI(4)P was detected in cells after fixation and immunofluorescence detection with anti-PI(4)P antibody. Each experiment was repeated three times.

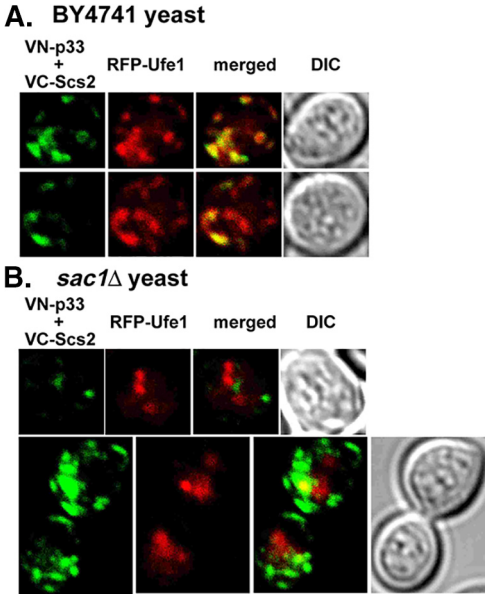

FIG 10 Ufe1 SNARE recruitment into vMCSs is inhibited in *sac1*Δ yeast. (A and B) Confocal microscopy images showing colocalization of RFP-Ufe1 with the BiFC signal from VN-p33 and VC-Scs2, which marks vMCSs, in WT and *sac1*Δ yeasts, respectively. Note that the yeast cells did not express $p92^{pol}$ and repRNA. Each experiment was repeated three times.

To confirm the biological significance of the lack of Rab5-positive endosome recruitment to the replication compartment in *sac1*Δ yeast, we visualized PE distribution in *sac1*Δ versus WT yeasts replicating TBSV repRNA. Unlike in WT yeast, in which PE is enriched within the large replication compartment decorated with GFP-p33 replication protein (Fig. 11C), the PE distribution was more dispersed in *sac1*Δ yeast, and PE was not enriched within the p33-decorated replication compartment (Fig. 11D). Based on these data, we propose that Sac1p plays a role in recruitment of Rab5-positive endosomes and thus facilitates PE enrichment at the sites of tombusvirus replication, which is required for efficient tombusvirus replication.

Sac1p is required for the efficient recruitment of several host factors into the replicase complex. The CFE-based *in vitro* replicase assembly experiments showed low TBSV replicase activity when the CFE was obtained from *sac1*Δ yeast, which might be the consequence of poor replicase assembly. Therefore, we decided to test the protein composition of the purified tombusvirus replicase, which has many co-opted cellular cofactors. Western blot analyses were performed on the detergent-solubilized affinity-purified tombusvirus replicase to detect the amounts of known co-opted cellular proteins in preparations obtained from *sac1*Δ or WT yeasts. This proteomic approach revealed ~4- to 5-fold-reduced amounts of co-opted Rpn11 deubiquitinase/metalloprotease and Cdc34 E2 ubiquitin-conjugating enzyme and ~3 times less Rad6p and Ubc2 E2 ubiquitin-conjugating enzymes, whereas Ded1p DEAD box helicase and Vps4 AAA ATPase were present in the purified replicase from *sac1*Δ yeast only at ~50 to 60% of the WT level (Table 1). The co-opted Cdc34p, Rad6p, Ubc2p, and Vps4p proteins are critical factors during VRC assembly (77–79), whereas Rpn11p and Ded1p affect the activities of VRCs, including viral (+)RNA synthesis and viral RNA recombination (80–82). Therefore, the reduced recruitment of these cellular factors into tombusvirus VRCs in *sac1*Δ versus WT yeasts could contribute to the serious defect in viral RNA accumulation in *sac1*Δ yeast. On the other hand, Sac1p does not seem to affect the recruitment of Vap27-1 VAP and Osh6p ORP proteins, which are components of virus-induced vMCSs (39), suggesting that these components associate directly with p33 replication protein to promote the formation of vMCSs. Altogether, our data suggest that Sac1p affects the assembly of the tombusvirus replicase by facilitating the recruitment of several host proteins into the VRCs.

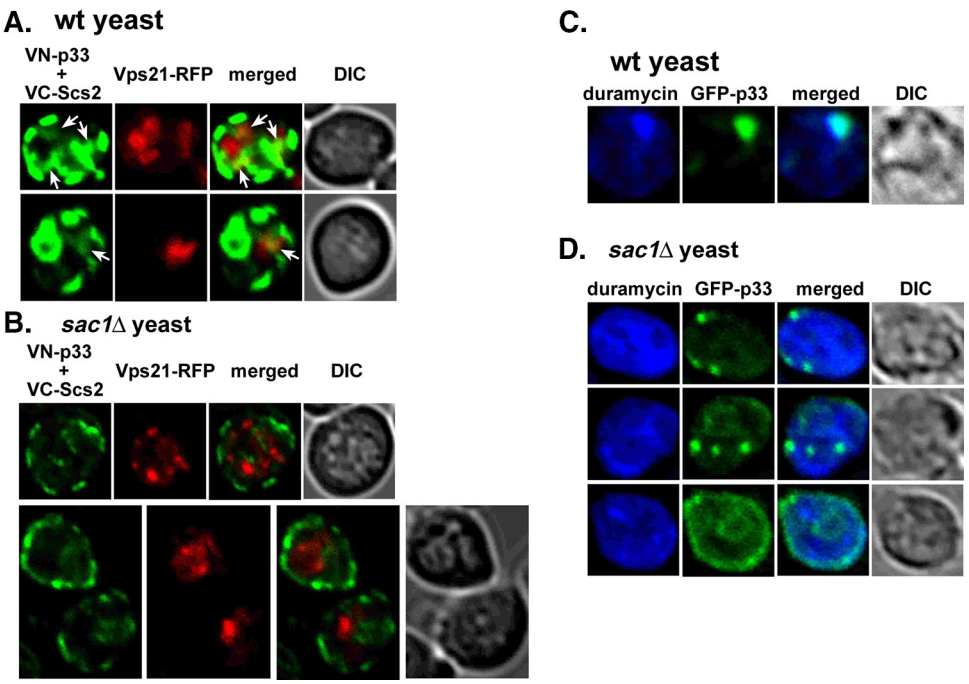

FIG 11 The yeast Rab5 protein is not recruited into vMCSs in *sac1*Δ yeast. (A and B) Confocal microscopy images showing colocalization of the Vps21-RFP (Rab5 homolog) with the BiFC signal from VN-p33 and VC-Scs2, which marks vMCSs, in WT and *sac1*Δ yeasts, respectively. Note that the yeast cells did not express $p92^{pol}$ and repRNA. Each experiment was repeated twice. (C) Enrichment of PE phospholipid, visualized with duramycin, within the GFP-p33-decorated viral replication compartment in WT yeast detected by confocal microscopy. The yeast also coexpressed $p92^{pol}$ and repRNA to support TBSV replication. (D) Lack of enrichment of PE phospholipid, visualized with duramycin, within the GFP-p33-decorated viral replication compartment in *sac1*Δ yeast detected by confocal microscopy. The yeast also coexpressed $p92^{pol}$ and repRNA to support TBSV replication. Each experiment was repeated three times.

DISCUSSION

High-throughput screening of the yeast knockout library has led to the identification of Sac1p PI(4)P phosphatase as one of the proviral cellular factors in TBSV replication in yeast (40). In this paper, we have confirmed that the yeast Sac1p and the orthologous Sac1a and Sac1b isoforms in *N. benthamiana* plants are important proviral factors during TBSV replication. TBSV replicase reconstitution experiments in CFEs from Sac1p-depleted yeast revealed that both minus- and plus-strand syntheses were inhibited,

TABLE 1 Host proteins copurified with p33 from *sac1*Δ yeast

Protein[a]	% (±SE)[b]
Bro1, ESCRT associated	141
Ded1 helicase	58 ± 7
Cdc34 E2 enzyme	28 ± 11
Osh6 ORP	92 ± 25
Pbp2 RNA binding	130 ± 14
Rad6 E2	32
RH2 helicase (eIF4AIII)	113 ± 44
Rpn11 deubiquitinase	22 ± 6
Tdh2 GAPDH	121 ± 14
Tef1 eEF1A	104 ± 3
Ubc2 E2	36
Vap27-1 (Scs2-like)	144 + 37
Vps4 AAA+ ATPase	49 + 13
Vps23 ESCRT I	152 ± 19

[a]The table lists the co-opted host proteins, which were expressed as well in *sac1*Δ yeast as in WT (BY4741) yeast based on the total protein samples (prior to purification). Co-opted host proteins copurified with p33 in lesser amounts from *sac1*Δ yeast are shown in boldface.

[b]Copurification of the given host protein with Flag-tagged p33 replication protein from WT yeast was taken as 100%. The standard error (SE) was calculated based on the results of three separate experiments.

pointing toward deficiency in the assembly of the TBSV replicase when Sac1p is limited. The role of Sac1p seems to be direct, based on the interaction with the p33 replication protein and the copurification of Sac1p with the tombusvirus replicase from yeast.

Sac1p is recruited into the virus-induced vMCSs to facilitate enrichment of sterols within the viral replication compartment. Based on the known cellular function of Sac1p in cellular MCSs, where Sac1p facilitates the directional transport of sterols from the ER to the PM or Golgi membrane with the help of PI(4)P (47–51), we analyzed in detail if Sac1p might also be recruited to the virus-induced vMCSs. Accordingly, we found that Sac1p is recruited to vMCSs, based on confocal and BiFC analyses. In addition, the amounts of Sac1p and Osh6 and Osh7 proteins copurified with Scs2 VAP protein, a known ER-resident tethering protein in the MCS (43), are increased in yeast replicating TBSV repRNA versus yeast lacking viral components (Fig. 5E). Moreover, we did not observe the characteristic enrichment of ergosterols within the viral replication compartment in yeast lacking the *SAC1* gene (Fig. 5C). These data support the model that TBSV stabilizes vMCSs, as indicated by the enhanced level of interactions among co-opted cellular vMCS components. The vMCSs then facilitate efficient sterol enrichment within the viral replication compartment (Fig. 12). Sterols are important cofactors and bind to the TBSV p33 replication protein (25), which is the master regulator of VRC assembly and viral (+)RNA recruitment into VRCs (25, 83). Enrichment of sterols within VRC membranes is also required to build tombusvirus VRCs resilient to the antiviral activity of the cellular RNA interference (RNAi) pathway (84).

Based on the retargeting of Sac1 into the CIRV-induced replication compartment, which consists of aggregated mitochondria, and the interaction between the cellular Sac1 and the CIRV p36 replication protein, we propose that CIRV also co-opts Sac1 functions to build its replication compartments.

PI(4)P phosphoinositide is a critical host factor during tombusvirus replication. The known substrate of Sac1p is PI(4)P, which is a minor, yet essential, component of the cytosolic leaflet of Golgi and plasma membranes (53, 85). The presence of PI(4)P in membranes facilitates the recruitment of PI(4)P-binding proteins, including Sac1p. These in turn promote the assembly of macromolecular complexes and initiate membrane trafficking and actin dynamics. Accordingly, we found a major proviral function(s) for PI(4)P during tombusvirus replication. This conclusion is supported by the findings that (i) depletion of two PI(4)P kinases, namely, Stt4p and Pik1p, in yeast or chemical inhibition of PI(4)P kinases in plant protoplasts decreased tombusvirus replication in cells; (ii) PI(4)P is present within the viral replication compartment, based on colocalization studies; and (iii) depletion of free PI(4)P via expression of the DrrA effector (from *Legionella*) inhibited the enrichment of PI(4)P within the replication compartment in yeast and plant cells. However, Sac1p converts PI(4)P to PI in the ER membrane, suggesting that the role of PI(4)P is likely temporal during tombusvirus replication. Altogether, the data presented firmly establish that both Sac1 and its substrate, PI(4)P, are required for TBSV replication in yeast and plants.

Sac1p affects PE enrichment in VRCs. The proviral role of Sac1p, however, does not seem to be restricted only to sterol enrichment in the viral replication compartment via vMCSs. We also showed that deletion of *SAC1* leads to deficiency in recruitment of several host factors, including the p33-driven hijacking of Rab5-decorated endosomes that deliver PE-rich membranes for robust viral replication (Fig. 12) (26, 38). Indeed, we found that Rab5 (Vps21p in yeast) is not recruited into vMCSs and PE is not enriched at the sites of replication in *sac1*Δ yeast (Fig. 11). The p33-containing punctate structures, which represent the sites of TBSV replication, are small in *sac1*Δ yeast cells in comparison with those formed in WT yeast (Fig. 12B). This is likely due to the lack of membrane proliferation and the lack of recruitment of Rab5-positive endosomes into the viral replication compartment. Accordingly, *in vitro* TBSV replicase assembly based on yeasts with deletion or depletion of Sac1p showed poor efficiency (Fig. 2), decreasing the production of both dsRNA replication intermediate and the (+)RNA progeny. Additional experiments will be needed to determine if the role of Sac1 is direct in the above-mentioned proviral processes.

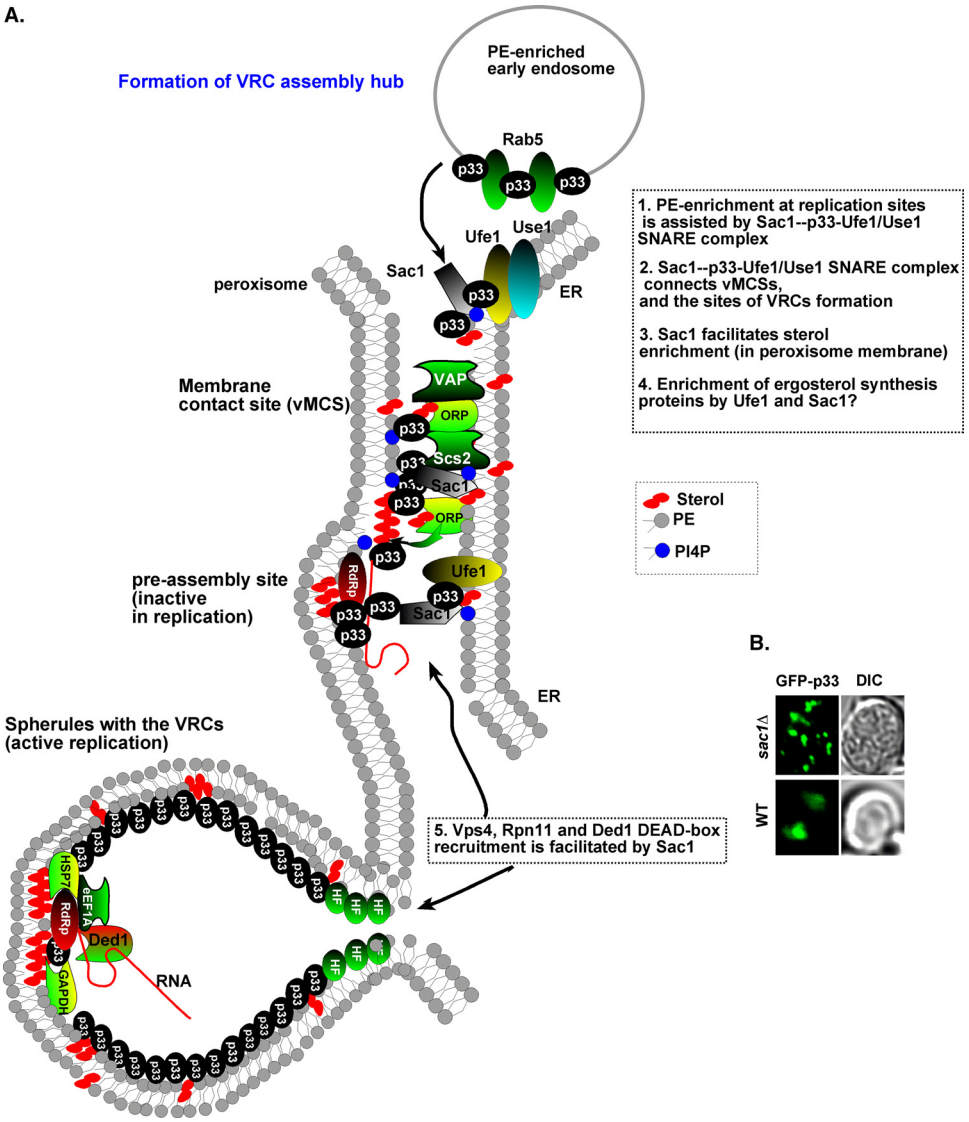

FIG 12 Model of the functional roles of the ER-resident Sac1 lipid phosphatase and PI(4)P in the biogenesis of the virus-induced replication compartment. (A) First, the co-opted Sac1, in collaboration with the ER-resident Scs2p VAP tethering protein and the cytosolic oxysterol binding proteins (ORP and Osh3, -5, -6, and -7 in yeast), participates in the formation of vMCSs between the ER and peroxisomes, which results in the enrichment of sterols and phospholipids in the peroxisomal membrane. Sac1 likely utilizes PI(4)P by converting it to PI in the ER to allow unidirectional transport, as shown in regular MCSs in healthy cells. Second, Sac1 promotes the preassembly of VRCs on the altered peroxisomal membrane by helping the abundant p33 replication protein of TBSV in the assembly process. The co-opted Sac1 facilitates the recruitment of Rab5 (Vps21)-positive endosomal structures and additional proviral host factors, such as the ER-resident syntaxin18-like Ufe1 SNARE, Vps4 AAA ATPase ESCRT protein, Rpn11 deubiquitinase, and Ded1 DEAD box RNA helicase. Sac1 might function in the second process in a complex with the viral replication protein and Ufe1 SNARE protein, which is part of the ERAS with Use1 SNARE protein, by constituting a VRC assembly hub. The possible organizing role of Sac1 in the actin network is not shown here. Note that the model is simplified here to clearly illustrate the roles of Sac1 and PI(4)P. Overall, by subversion of Sac1, PI(4)P and the additional host components for proviral functions allow tombusviruses to build nuclease- and protease-insensitive virus replication compartment (only one spherule is shown for simplicity). (B) Confocal microscopic images showing the small viral replication compartments decorated by GFP-p33 in yeast lacking Sac1 lipid phosphatase. The yeast also coexpressed $p92^{pol}$ and repRNA to support TBSV replication.

Sac1p might also function as a scaffold protein and assembly platform to facilitate rapid generation of VRCs. Tombusviruses are successful pathogens of plants due to their ability to replicate rapidly and efficiently in infected cells. These viruses can quickly assemble VRCs for robust replication (84). The intensive assembly of large virus-induced membranous structures likely depends not only on protein and

RNA chaperones, such as Hsp70 and eEF1A (63, 86), but also on scaffolding proteins, which bring several proteins and membranes together for rapid assembly. Based on the current work, it seems that Sac1p might act as a scaffolding protein, possibly for vMCS stabilization and during TBSV VRC assembly. Accordingly, the co-opted protein composition of the TBSV replicase is dramatically different in *sac1*Δ yeast (Table 1).

In collaboration with Ufe1 SNARE protein, Sac1 is a component of the TBSV replicase assembly hub. Surprisingly, we found that, in the absence of Sac1p, TBSV cannot efficiently hijack the ER-resident Ufe1p SNARE protein. Ufe1p is a major component of the ERAS in the ER subdomain, which serves as an assembly hub for several tombusvirus VRC components and greatly affects the formation of the viral replication compartment (38). We propose that subversion of the ER-resident Sac1 helps TBSV to hijack Ufe1 and the ERAS subdomain of the ER (Fig. 12). Thus, on one hand, by co-opting Sac1, TBSV gains access to local manipulation and enrichment of membrane lipids in vMCSs and ultimately in VRCs. On the other hand, the subverted Sac1 serves as an assembly platform that accelerates the efficient generation of numerous VRCs in infected cells. Accordingly, confocal microscopic analysis of *sac1*Δ yeast revealed tiny p33 replication protein-containing foci (punctate structures) (Fig. 12B) instead of the large punctate structures that are representative of the tombusvirus replication compartments (32, 87). This suggests a lack of discrete viral replication compartment formation in *sac1*Δ yeast. The co-opted Sac1 is unlikely to perform all these proviral functions by itself, but instead, as a component of different protein complexes, such as with the syntaxin18-like Ufe1 SNARE protein-p33 replication protein complexes. Altogether, the data presented are in agreement with a model in which the co-opted Sac1 plays a significant role in the formation of the tombusvirus replication compartment by bringing together vMCSs to obtain optimal lipid composition in the subverted membranes and aggregated peroxisomes, where numerous spherules/VRCs could then efficiently form. Thus, the several proviral roles of Sac1 illustrate that vMCS formation and the assembly of VRCs are likely linked, as in the model shown in Fig. 12A. These "VRC assembly hub" functions of Sac1 and Ufe1 could facilitate the sequestering and concentration of the viral replication proteins and several co-opted host proteins and critical lipids within the limited ERAS subdomains within the ER membranes. We propose that by targeting Sac1 and Ufe1 SNARE protein (and other components of the ERAS), TBSV generates an efficient VRC assembly hub that includes the ERAS subdomain of the ER and vMCS with peroxisomes (Fig. 12A).

Since (+)RNA viruses remodel subcellular membranes to facilitate virus replication and avoid antiviral responses (4–6, 10, 88, 89), it is possible that Sac1 lipid phosphatase and exploitation of MCSs could be widespread among viruses. Indeed, several animal (+)RNA viruses, such as picornaviruses, are known to depend on PI(4)P and Sac1 for replication (6, 85). Poliovirus (PV) and coxsackievirus B3 hijack the Golgi and *trans*-Golgi network (TGN) membranes and cellular PI4K to their replication organelles to produce PI(4)P *in situ* (11, 85, 90, 91). The PI(4)P-enriched membranes then recruit cellular PI(4)P-binding proteins to aid viral replication. The 3C replication protein of picornaviruses binds directly to PI(4)P to support viral RNA synthesis (90, 92). PI(4)P is also required for sterol enrichment within the replication organelles of rhinovirus, Aichi virus, and PV (93–95). Co-opted cellular PI4K kinases and oxysterol-binding proteins are also important for HCV replication (91, 96–98). In addition to viruses, several intracellular bacterial pathogens also hijack Sac1, PI(4)P, and MCSs to support the pathogenesis process (99). Therefore, it will be interesting to learn if other viruses and pathogens could also exploit Sac1 lipid phosphatase for many functions, as tombusviruses do. Altogether, Sac1 seems to be a possible target for antiviral approaches.

MATERIALS AND METHODS

Yeast strains and expression plasmids. *Saccharomyces cerevisiae* strains BY4741 (*MAT***a** *his3*Δ*1 leu2*Δ*0 met15*Δ*0 ura3*Δ*0*) and R1158 (100), BY4741 *sac1*Δ (BY4741 *sac1*Δ::*kanMX4*), BY4741 Lsb6Δ (BY4741 *lsb6*Δ::*kanMX4*), TET::PIK1, and TET::STT4 (yTHC library) were obtained from Open Biosystems. A yeast expression plasmid, pRS406-PHO5-GFP-hFAPP1-PH, was obtained from Addgene. Yeast strain NMY51 was obtained from Dualsystems. Yeast strains SEY6210 (*MAT***a** *ura3-52 his3*Δ*200 lys2-801 leu2-3,112*

*trp1*Δ*901 suc2*Δ*9*) and JRY6232 (SEY6210 *osh5*Δ::*LEU2 osh6*Δ::*LEU2 osh7*Δ::*HIS3*) were obtained from Christopher T. Beh (Simon Fraser University).

To generate yeast strain JRY6232 *his3*Δ, the *KanMX4* gene was PCR amplified from plasmid pYM45 (European *Saccharomyces cerevisiae* Archive for Functional Analysis [EUROSCARF]) (101) using primers 5489 (ATGACAGAGCAGAAAGCCCTAGTAAAGCGTATTACAAATGAAACGTACGCTGCAGGTCGA) and 5490 (CTACATAAGAACACCTTTGGTGGAGGGAACATCGTTGGTACCATCGATGAATTCGAGCTC). The PCR product was used for transformation that created strain SEY6210 (*osh5*Δ::*LEU2 osh6*Δ::*LEU2 osh7*Δ::*KanMX4 his3*Δ). BY4741-based SAC1::GAL1-6×HA-Sac1-Nat (referred to here as GAL1::SAC1) and OSH7::GAL1-6×HA-Osh7-Nat (OSH7-6×HA) yeast strains expressing 6×HA-tagged Sac1p or 6×HA-tagged Osh7p, respectively, under the *GAL1* promoter from their natural chromosomal locations, were created by using plasmid pYM-N32 from the EUROSCARF plasmid collection according to the authors' recommendation (101). The *scs2*Δ *scs22*Δ double-mutant (BY4741 *SCS2*::*kanMX SCS22*::*hphNT1*) strain was created from BY4741 *scs2*Δ (BY4741 *SCS2*::*kanMX*) (Open Bioystems) by using plasmid pFA6a-hphNT from the EUROSCARF plasmid collection (101).

The following yeast expression plasmids have been previously described: pGAD-LEU-Cup1-His92 (102), pESC-URA-Cup1-His92 (31), pGBK-HIS-Cup1-His33/ADH1-DI72 (65), pGBK-HIS-Gal1-RFP33/Gal1-DI72 (26), pDest-565-DrrA (35), and RFP-MS2-CP and DI72-MS2CP (66).

Plant expression plasmids. Plant expression construct pGD-hFAPP1-PH was created by cloning hFAPP1-PH fragments PCR amplified from pRS406-PHO5-GFP-hFAPP1-PH (Addgene) with the primer pairs GFP-FAPP1-PH/XbaI/F (TGCATCTAGAATTCGAATATAATGTCTAAAGGAGAAGAACTTTTCACTGG) and GFP-FAPP1-PH/PstI/R (TGCACTGCAGTCATGTATCAGTCAAACATGCTTTGGAGC) into pGD-2x35Spro-L using XbaI and PstI sites. The full-length sequence of AtSAC1 was PCR amplified with primer pairs 7644 (ACGCGGATCCATGGCGAAATCGGAAAACTCAACG) and 7645 (ACGCGTCGACTTACTGCAGAATGACCTTCGG GACCTTATCATCTC) using *A. thaliana* cDNA as the template. The PCR product was digested with BamHI and SalI and then ligated into pGD-35S-GFP, pGD-35S-RFP, and pGD-35S-nYFP (the N-terminal domain of yellow fluorescent protein [YFP]) vectors.

The following plant expression plasmids have been previously described: pGD-p33-RFP, pGD-p33-GFP, pGD-p33-BFP, and pGD-RFP-SKL (26, 30, 67) and pEarleyGate100-DrrA (35).

Wild-type and RFP-H2b transgenic *N. benthamiana* plants were potted in soil and placed in a growth room at 25°C under a 16-h light/8-h dark cycle.

Analysis of tombusvirus replication in yeast. Tombusvirus replication was analyzed in BY4741 and BY4741 *sac1*Δ yeast strains. These yeast strains were transformed with LpGADCUP1-p92 and HpGBKCUP1-p33/ADH1-DI-72 to express the p33 and p92 viral proteins, along with the DI-72 repRNA. The yeasts were grown in synthetic complete medium lacking leucine and histidine (SC-LH$^-$ medium) supplemented with 2% glucose containing 50 μM $CuSO_4$ to induce viral protein expression. Yeasts were harvested after 16 and 48 h, and total RNA was extracted. Northern blot analysis was performed with a 3′-end-specific repRNA probe to detect the repRNA accumulation level, and an rRNA-specific probe was used to observe the rRNA level as described previously (61). Viral protein p33 and p92 expression was detected by Western blotting using anti-His antibody (103). In the complementation assay, yeast strains were transformed with plasmids LpGADCUP1-p92 and HpGBKCUP1-p33/ADH1-DI-72, and UpYC-GAL1-HisSac1. Yeasts were grown in synthetic complete medium lacking uracil, leucine, and histidine (SC-ULH$^-$ medium) containing 2% glucose and 100 μM bathocuproine disulfonate (BCS) overnight. BCS inhibits the expression of the viral proteins driven by the *CUP1* promoter. Then, the yeasts were grown in SC-ULH$^-$ medium containing 2% raffinose or galactose in the presence of BCS for 12 h. The BCS was washed out, and fresh SC-ULH$^-$ medium supplemented with 2% raffinose or galactose containing 50 μM $CuSO_4$ was added to induce viral protein expression for 24 h. Northern blotting and Western blotting were done as described above.

The *osh5*Δ *osh6*Δ *osh7*Δ triple-mutant SEY6210 and WT SEY6210 yeast strains were transformed to express HA-tagged Sac1p under the *GAL1* promoter from the chromosome using plasmid pYM-N32 from the EUROSCARF plasmid collection (101). Then, both strains were transformed with plasmids LpGADCUP1-p92 and HpGBKCUP1-p33/ADH1-DI-72. Cells were grown in SC-LH$^-$ medium supplemented with 2% glucose in the presence of 100 μM BCS overnight. Then, the cells were grown in SC-LH$^-$ medium supplemented with either 2% raffinose or 2% galactose in the presence of BCS for 12 h. Finally, the BCS was washed out, and fresh SC-LH$^-$ medium supplemented with 2% raffinose or 2% galactose containing 50 μM $CuSO_4$ was provided for 24 h. Northern blotting and Western blotting were done as described above.

To test the effect of yeast PI(4)P kinases on TBSV replication, we transformed BY4741 and *lsb6*Δ yeasts with pGAD-LEU-Cup1-His92, pGBK-HIS-Cup1-His33/ADH1-DI-72, and pESC-URA-Empty plasmids. In the cases of TET::STT4 and TET::PIK1 yeast strains, the transformation was done with plasmids pGAD-LEU-Cup1-His92 and pGBK-HIS-Cup1-His33/ADH1-DI-72. The transformed BY4741, *lsb6*Δ, TET::STT4, and TET::PIK1 yeasts were cultured in SC-ULH$^-$ medium supplemented with 2% glucose and 100 μM BCS at 29°C for 16 h, and then the yeasts were continuously cultured in SC-ULH$^-$ medium supplemented with 2% galactose and 50 μM $CuSO_4$ at 29°C for 16 h. To deplete the targeted proteins in TET::STT4 and TET::PIK1 yeast strains, 10 μg/ml doxycycline was added to both the pregrowth medium and the incubation medium. After harvest, RNA and protein were analyzed as described above.

Analysis of TBSV replication in *N. benthamiana* protoplasts. Isolation of protoplasts from *N. benthamiana* leaves were carried out as described previously (26). The isolated protoplasts were transfected with TBSV genomic RNA isolated from infected plants using polyethylene glycol (PEG) (104) and treated with 50 μM PAO, a PI4K inhibitor (72, 73). Sixteen hours after transfection, the protoplasts were harvested by centrifugation and analyzed for TBSV levels by Northern blotting analysis.

Confocal laser microscopy analysis of yeast cells. To analyze the subcellular localization of PI(4)P, plasmid pRS406-PHO5-GFP-hFAPP1-PH, along with pESC-TRP-Cup1-His92, pGBK-HIS-Gal1-RFP33/ADH1-DI72, and pAG415-DrrA or pAG415-Empty, was transformed into yeast strain SEY6210. The transformed yeasts were grown under the conditions used in TBSV RNA analysis as described above. The confocal images were obtained sequentially with an Olympus FV1000 microscope (Olympus America) and merged using Olympus FLUOVIEW 1.5 software (22).

Colocalization and BiFC assay in yeast. WT BY4741 and BY4741 *sac1*Δ strains were transformed with UpRS426-GFP-Sac1 (provided by Daniel Barajas), along with HpESC-GAL1-BFP-p33 (26). The transformed yeasts were grown in UH$^-$ minimal medium supplemented with 2% glucose for 12 h, and then yeast cells were harvested and washed and the medium was changed to SD-UH$^-$ minimal medium supplemented with 2% galactose. GFP-Sac1 expression was driven by its endogenous promoter present on the pRS426 plasmid. Cells were harvested and washed after 24 h. Then, 2 to 3 μl of cell suspension was dropped on poly-L-lysine-coated slides and visualized with a laser scanning microscope (39). Single frames were obtained.

A BiFC assay was carried out as described previously (38, 39). Briefly, BY4741 and *sac1*Δ strains were transformed with HpESC-nYFP-p33-DI72 and UpYC-cYFP-SCS2, along with the LpGAD-ADH1-CFP-Sac1, LpRS315-TEF1-RFP-Vps21, or LpGAD-ADH1-RFP-Ufe1 plasmid (26, 38). Interaction between TBSV nYFP-p33 replication protein and the Scs2-cYFP (the C-terminal domain of YFP) protein and colocalization with cyan fluorescent protein (CFP)-Sac1p was detected by growing transformed yeast colonies in liquid yeast minimal synthetic drop-out (SD) medium containing 2% galactose for 24 h at 29°C, followed by confocal laser microscopy.

Detection of PE distribution in yeasts. The distribution of PE was studied in BY4741 WT and BY4741 *sac1*Δ yeast strains as described previously (30). GFP-p33 protein was expressed form the pRS425-pCUP1-GFP-p33 plasmid. Yeast cells were grown in SC-L$^-$ medium supplemented with 2% glucose in the presence of 100 μM BCS overnight. Then, the BCS was washed out and fresh SC-L$^-$ medium supplemented with 2% glucose containing 50 μM $CuSO_4$ was provided to induce GFP-p33 expression. After 16 h, yeast cells were harvested, and PE distribution was detected by using biotinylated duramycin peptide and streptavidin conjugated with Alexa Fluor 405 (30).

Ergosterol distribution in yeasts. To examine ergosterol distribution, the BY4741 yeast strain was cotransformed with plasmids HpESC-GAL1-RFP-p33 and UpRS426-GFP-Sac1. The control strain was transformed with empty pESC and UpRS426-GFP-Sac1. The yeast strains were grown in SC minimal medium supplemented with 2% galactose for 24 h at 23°C. The yeast cultures were fixed with 3% formaldehyde for 1 h at room temperature. The formaldehyde was quenched by addition of glycine (0.1 M final concentration). The fixed cells were centrifuged and washed twice with distilled water. The washed cells were incubated with 5 mg/ml filipin complex (Sigma Chemicals) in the dark for 15 min at 23°C. Filipin-based fluorescence was observed by spotting 2 to 3 μl of the cell suspensions onto poly-L-lysine-coated microscope slides under a UV light microscope using a DAPI (4′,6-diamidino-2-phenylindole) filter (39).

Analysis of protein interactions *in vivo* using a yeast membrane two-hybrid assay. The MYTH assay was done as previously described (39). Briefly, to determine the interaction between *S. cerevisiae* Sac1p (ScSac1p) and p33 replication protein, plasmid pGAD-BT2-N-His33 was transformed with one of the following plasmids: pPR-N-RE, pPR-N-RE-ssa1, pPR-N-RE-ScSac1, pPR-N-RE-ScOsh5, pPR-N-RE-ScOsh6, or pPR-N-RE-ScOsh7. Similar amounts of transformed yeast colonies were picked up and suspended in 100 μl water, 8 μl of which was cultured on TL$^-$ plates (SD agar plates lacking threonine and leucine) as a loading control or on TLHA$^-$ plates (SD agar plates lacking threonine, leucine, histidine, and adenine) to score protein interactions.

Virus-induced gene silencing of *SAC1* genes in *N. benthamiana*. Three *SAC1*-like genes were identified in *A. thaliana*: *AtSAC1a* (At3g51830), *AtSAC1b* (At5g66020), and *AtSAC1c* (At3g51460), which can rescue the cold-sensitive and inositol auxotroph yeast *sac1*-null mutant strain. These proteins are localized in the ER (59). The translation product of *AtSAC1a* showed 60% similarity to the *S. cerevisiae* Sac1p (59). To find *N. benthamiana*-specific *SAC1* sequences, we performed a BLAST search in the TGI database (Gene Indices, Harvard University) using the sequences of *AtSAC1a*, *AtSAC1b*, and *AtSAC1c* against *N. benthamiana* TC sequences. The BLAST search of *SAC1b* and *SAC1c* resulted in the same hit, TC141032, with 72% identity with the *Arabidopsis* sequences. *SAC1a* resulted in a separate hit, TC148342. We designed primers based on the *N. benthamiana* sequences to PCR amplify a 474-bp (SAC1a) and a 398-bp (SAC1b) fragment to create the VIGS vectors, pTRV2-SAC1A*Nb* and pTRV2-SAC1BNb. The primer pairs for PCR were as follows: 5960F (CGCCGGATCCGGGTGGATCAAGGTGATGAA)/5961R (CGCCTCGAGT GCCTTCCATTTGCTTTGA) and 5962F (CGCCGGATCCGGTGGATGGGTCAATGAAAC)/5963R (CGCCTCGAGGA GGGTCTGCTTGTCTCCAC), respectively. VIGS in *N. benthamiana* was performed as described previously (105). Briefly, *Agrobacterium* cultures were transformed with plasmid pTRV2-SAC1A*Nb*, pTRV2-SAC1B*Nb*, or pTRV2-cGFP as a control. *N. benthamiana* plants were agroinfiltrated (optical density at 600 nm [OD_{600}], 0.5). On the 8th day of agroinfiltration, leaves were sap inoculated with TBSV. Then, total RNA was extracted on the 2nd day postinoculation from the infected leaves, followed by Northern blotting analysis. Silencing of the target genes was confirmed with reverse transcription (RT)-PCR using primers 5960F (CGCCGGATCCGGGTGGATCAAGGTGATGAA) and 6342 (GGCGTAGTTTCGTCCTCCTA) on total RNA extracts of pTRV2-SAC1ANb- and pTRV2-cGFP-agroinfiltrated plants. RT-PCR amplification of tubulin mRNA sequence was performed as a control (39).

Confocal microscopic analysis of plant cells. To analyze the subcellular localization of AtSac1 in the presence or absence of TBSV components in *N. benthamiana* leaves, we introduced plasmids pGD-35S-RFP-AtSac1, pGD-35S-T33-BFP, and pGD-35S-GFP-SKL (as a peroxisome marker) via agroinfiltration. The effect of CIRV on AtSac1 distribution in *N. benthamiana* leaves was studied by agroinfiltration of a mixture

of *Agrobacterium* transformants (strain C58C1) carrying plasmids pGD-35S-RFP-AtSac1, pGD-35S-C36-BFP, and pGD-35S-GFP-AtTim21 (as a mitochondrial marker). Then, TBSV or CIRV inoculation with sap was performed at 16 h postagroinfiltration. At 2.5 days postagroinfiltration, the agroinfiltrated leaves were subjected to confocal laser microscopy.

To demonstrate if AtSac1 is recruited into an active virus replication compartment, a modified repRNA carrying six repeats of a hairpin RNA from the MS2 bacteriophage, which is specifically bound by its coat protein, was utilized (66). *N. benthamiana* leaves were coinfiltrated with different combinations of agrobacteria carrying pGD-p33-BFP (OD_{600}, 0.3), pGD-GFP-AtSac1 (OD_{600}, 0.3), pGD-RFP-MS2-CP (OD_{600}, 0.5), pGD-p19 (OD_{600}, 0.3), pGD-(+)DI72-MS2hp (OD_{600}, 0.5), and pGD-CNV-20K (OD_{600}, 0.4). Then, the samples were subjected to confocal microscopic analysis at 3.5 days postagroinfiltration.

To detect interaction between AtSac1 and TBSV p33 or CIRV p36 replication protein, we performed BiFC assays. Plasmids pGD-T33-cYFP, pGD-C36-cYFP, pGD-C-cYFP (as a negative control), pGD-nYFP-AtSac1, pGD-nYFP-MBP (as a negative control), pGD-RFP-SKL (as a peroxisome marker), and pGD-RFP-AtTim21 (as a mitochondrial marker) were separately transformed into the *Agrobacterium* strain C58C1. The *Agrobacterium* transformants with different combinations were used to infiltrate *N. benthamiana* leaves, which were harvested and then subjected to confocal microscopic analysis at 2 days after agroinfiltration.

To observe the colocalization of p33 and PI(4)P in the presence or absence of the *Legionella* DrrA effector in *N. benthamiana* epidermal cells, pGD-p33-RFP, pGD-p19 pEarlygate-DrrA, and pGD-GFP-hFAPP1-PH were agroinfiltrated into *N. benthamiana* leaves, and the infiltrated leaves were inoculated with TBSV 1 day after the agroinfitration. Images were taken 2 days after infiltration. To visualize PI(4)P distribution in plant cells, mesophyll protoplasts were isolated from *N. benthamiana* leaves 1 day after agroinfiltration with pGD-p19, pGD-p33-GFP, or pGD-p33-BFP, and pEarlygate-DrrA as described above. The protoplasts were transfected with TBSV genomic RNA using PEG (104). Sixteen hours after transfection, protoplasts were harvested, fixed with 2% paraformaldehyde, and applied to a poly-L-lysine–coated slide. Using mouse anti-PI(4)P IgM (Echelon; Z-P004) and Alexa 568-conjugated anti-mouse secondary antibody (Invitrogen), PI(4)P distribution was analyzed with confocal microscopy (22).

Recombinant-protein purification from *E. coli*. For the expression and purification of the recombinant MBP-tagged TBSV p33 and p92 replication proteins from *E. coli*, we followed a published protocol (106).

***In vitro* TBSV replication assay in cell-free yeast extract.** BY4741 and GAL1::Sac1 yeast strains were pregrown for 16 h at 29°C in yeast extract-peptone-glucose (YPG) medium supplemented with 2% raffinose. After the yeast cells were centrifuged at 3,000 rpm for 5 min and washed with yeast extract-peptone-dextrose (YPD) medium, the yeasts were grown for 8 h at 29°C in YPD medium. We followed a previously published protocol (63, 107) for the preparation of CFEs to reconstitute the TBSV replicase *in vitro*. The *in vitro* TBSV replication assays were performed in 20-μl total volumes containing 3 μl of CFE, 0.25 μg DI-72 (+)repRNA transcript, 200 ng purified MBP-p33, 200 ng purified MBP-$p92^{Pol}$, and the CFE buffer. After incubation at 25°C for 3 h, the RNA products synthesized in the replication assays were separated by electrophoresis in 0.5× Tris-borate-EDTA buffer in a 5% polyacrylamide gel containing 8 M urea.

In the second TBSV replication assay, the membrane and soluble fractions of CFEs from BY4741 and *sac1*Δ yeasts were separated via centrifugation at 16,000 rpm. The BY4741 and *sac1*Δ strains were pregrown in YPD medium for 16 h, and then fresh YPD medium was supplied for an additional 6 h. After mixing the membrane and soluble fractions in different combinations, the *in vitro* TBSV replication assays were performed as described previously (63, 107).

Copurification of various host proteins and p33 from yeasts. For the copurification of chromosomally expressed 6×HA-tagged Sac1p with tombusvirus Flag-p33 replication protein, the GAL1::SAC1 yeast strain was transformed with plasmids pGBK-His33-CUP1/DI72-GAL1 or pGBK-Flag33-CUP1/DI72-GAL1 and pGAD-CUP1-His92. For copurification of His_6-tagged Osh7 and His_6-Sac1 proteins with tombusvirus Flag-p33 replication protein, BY4741 and *scs2*Δ *scs22*Δ double-mutant yeast strains were cotransformed with plasmid pESC/DI72/His33 or pESC/DI72/FLAG33, pGAD-His92, and pYC2/NT-C plasmids expressing His_6-tagged Osh7p and His_6-Sac1p. For copurification of Flag-tagged Scs2p and His_6-tagged Osh5p, His_6-Osh6p, His_6-Osh7p, and His_6-Sac1p, BY4741 yeast was transformed with HpESC-Flag-Scs2, together with pYC2/NT-C plasmid expressing one of the His_6-tagged proteins. Control yeast samples were transformed with plasmid coding for YFP-tagged Scs2. Flag-based purification was carried out as described previously (39).

BY4741 and *sac1*Δ yeast strains were transformed with the following plasmids: pGBK-HIS-Cup-Flag33/Gal-DI-72 (108) expressing Flag-tagged p33 and the TBSV DI-72 repRNA; pGAD-LEU-Cup-Flag92 expressing Flag-tagged p92; and one of the UpESC-Cup-His plasmids expressing His_6-Bro1p, His_6-Ded1p, His_6-Cdc34p, His_6-Osh6p, His_6-Pbp2p, His_6-Rad6p, His_6-RH2, His_6-Rpn11p, His_6-Tdh2p, His_6-Tef1p, His_6-Ubc2p, His_6-Vap27-1, His_6-Vps4p, or His_6-Vps23p. The experiment was performed as described previously (38). Briefly, transformed yeasts were grown for 18 h in SC-ULH$^-$ medium supplemented with 2% galactose and 100 μM BCS at 29°C. Then, the medium was changed to SC-ULH$^-$ medium supplemented with 2% glucose and 100 μM BCS. After growing yeasts for 24 h at 29°C, the medium was changed to SC-ULH$^-$ medium containing 2% glucose and 50 μM $CuSO_4$, and culturing continued for 10 h at 23°C. Then, Flag-tagged replicase was purified following a previously published protocol (82). Fractions eluted from anti-FLAG M2-agarose affinity resin were balanced based on the amount of purified Flag-p33. Both total and purified fractions were analyzed for the presence of His_6-tagged host proteins. Purified Flag-p33 was detected by Western blotting using anti-Flag antibody; copurified His_6-tagged host proteins were detected with anti-His antibody, followed by anti-mouse antibody conjugated to alkaline phosphatase. Colorimetric detection was performed with nitroblue tetrazolium (NBT) and 5-bromo-4-chloro-3-indolylphosphate (BCIP).

ACKNOWLEDGMENTS

We thank Daniel Barajas for participating in the initial stage of this work. Members of the Nagy laboratory are thanked for their valuable comments. Yeast strain JRY6232 was obtained from Christopher T. Beh (Simon Fraser University).

This work was supported by the National Science Foundation (IOS-1922895) and a USDA hatch grant (KY012042) to P.D.N.

REFERENCES

1. Belov GA, van Kuppeveld FJ. 2012. (+)RNA viruses rewire cellular pathways to build replication organelles. Curr Opin Virol 2:740–747. https://doi.org/10.1016/j.coviro.2012.09.006.
2. den Boon JA, Ahlquist P. 2010. Organelle-like membrane compartmentalization of positive-strand RNA virus replication factories. Annu Rev Microbiol 64:241–256. https://doi.org/10.1146/annurev.micro.112408.134012.
3. Nagy PD, Pogany J. 2011. The dependence of viral RNA replication on co-opted host factors. Nat Rev Microbiol 10:137–149. https://doi.org/10.1038/nrmicro2692.
4. Wang A. 2015. Dissecting the molecular network of virus-plant interactions: the complex roles of host factors. Annu Rev Phytopathol 53:45–66. https://doi.org/10.1146/annurev-phyto-080614-120001.
5. Nagy PD. 2016. Tombusvirus-host interactions: co-opted evolutionarily conserved host factors take center court. Annu Rev Virol 3:491–515. https://doi.org/10.1146/annurev-virology-110615-042312.
6. Altan-Bonnet N. 2017. Lipid tales of viral replication and transmission. Trends Cell Biol 27:201–213. https://doi.org/10.1016/j.tcb.2016.09.011.
7. van der Schaar HM, Dorobantu CM, Albulescu L, Strating JR, van Kuppeveld FJ. 2016. Fat(al) attraction: picornaviruses usurp lipid transfer at membrane contact sites to create replication organelles. Trends Microbiol 24:535–546. https://doi.org/10.1016/j.tim.2016.02.017.
8. Shulla A, Randall G. 2016. (+)RNA virus replication compartments: a safe home for (most) viral replication. Curr Opin Microbiol 32:82–88. https://doi.org/10.1016/j.mib.2016.05.003.
9. Fernandez de Castro I, Tenorio R, Risco C. 2016. Virus assembly factories in a lipid world. Curr Opin Virol 18:20–26. https://doi.org/10.1016/j.coviro.2016.02.009.
10. Zhang Z, He G, Filipowicz NA, Randall G, Belov GA, Kopek BG, Wang X. 2019. Host lipids in positive-strand RNA virus genome replication. Front Microbiol 10:286. https://doi.org/10.3389/fmicb.2019.00286.
11. Hsu NY, Ilnytska O, Belov G, Santiana M, Chen YH, Takvorian PM, Pau C, van der Schaar H, Kaushik-Basu N, Balla T, Cameron CE, Ehrenfeld E, van Kuppeveld FJ, Altan-Bonnet N. 2010. Viral reorganization of the secretory pathway generates distinct organelles for RNA replication. Cell 141:799–811. https://doi.org/10.1016/j.cell.2010.03.050.
12. Schoggins JW, Randall G. 2013. Lipids in innate antiviral defense. Cell Host Microbe 14:379–385. https://doi.org/10.1016/j.chom.2013.09.010.
13. Perera R, Riley C, Isaac G, Hopf-Jannasch AS, Moore RJ, Weitz KW, Pasa-Tolic L, Metz TO, Adamec J, Kuhn RJ. 2012. Dengue virus infection perturbs lipid homeostasis in infected mosquito cells. PLoS Pathog 8:e1002584. https://doi.org/10.1371/journal.ppat.1002584.
14. Nagy PD, Pogany J. 2010. Global genomics and proteomics approaches to identify host factors as targets to induce resistance against Tomato bushy stunt virus. Adv Virus Res 76:123–177. https://doi.org/10.1016/S0065-3527(10)76004-8.
15. Nagy PD. 2008. Yeast as a model host to explore plant virus-host interactions. Annu Rev Phytopathol 46:217–242. https://doi.org/10.1146/annurev.phyto.121407.093958.
16. White KA, Nagy PD. 2004. Advances in the molecular biology of tombusviruses: gene expression, genome replication, and recombination. Prog Nucleic Acids Res Mol Biol 78:187–226. https://doi.org/10.1016/S0079-6603(04)78005-8.
17. Barajas D, Jiang Y, Nagy PD. 2009. A unique role for the host ESCRT proteins in replication of Tomato bushy stunt virus. PLoS Pathog 5:e1000705. https://doi.org/10.1371/journal.ppat.1000705.
18. McCartney AW, Greenwood JS, Fabian MR, White KA, Mullen RT. 2005. Localization of the tomato bushy stunt virus replication protein p33 reveals a peroxisome-to-endoplasmic reticulum sorting pathway. Plant Cell 17:3513–3531. https://doi.org/10.1105/tpc.105.036350.
19. de Castro IF, Fernandez JJ, Barajas D, Nagy PD, Risco C. 2017. Three dimensional imaging of the intracellular assembly of a functional viral RNA replicase complex. J Cell Sci 130:260–268. https://doi.org/10.1242/jcs.181586.
20. Xu K, Nagy PD. 2014. Expanding use of multi-origin subcellular membranes by positive-strand RNA viruses during replication. Curr Opin Virol 9:119–126. https://doi.org/10.1016/j.coviro.2014.09.015.
21. Nagy PD. 2017. Exploitation of a surrogate host, Saccharomyces cerevisiae, to identify cellular targets and develop novel antiviral approaches. Curr Opin Virol 26:132–140. https://doi.org/10.1016/j.coviro.2017.07.031.
22. Chuang C, Barajas D, Qin J, Nagy PD. 2014. Inactivation of the host lipin gene accelerates RNA virus replication through viral exploitation of the expanded endoplasmic reticulum membrane. PLoS Pathog 10:e1003944. https://doi.org/10.1371/journal.ppat.1003944.
23. Sharma M, Sasvari Z, Nagy PD. 2011. Inhibition of phospholipid biosynthesis decreases the activity of the tombusvirus replicase and alters the subcellular localization of replication proteins. Virology 415:141–152. https://doi.org/10.1016/j.virol.2011.04.008.
24. Sharma M, Sasvari Z, Nagy PD. 2010. Inhibition of sterol biosynthesis reduces tombusvirus replication in yeast and plants. J Virol 84:2270–2281. https://doi.org/10.1128/JVI.02003-09.
25. Xu K, Nagy PD. 2017. Sterol binding by the tombusviral replication proteins is essential for replication in yeast and plants. J Virol 91:e01984-16. https://doi.org/10.1128/JVI.01984-16.
26. Xu K, Nagy PD. 2016. Enrichment of phosphatidylethanolamine in viral replication compartments via co-opting the endosomal Rab5 small GTPase by a positive-strand RNA virus. PLoS Biol 14:e2000128. https://doi.org/10.1371/journal.pbio.2000128.
27. Pogany J, Nagy PD. 2015. Activation of tomato bushy stunt virus RNA-dependent RNA polymerase by cellular heat shock protein 70 is enhanced by phospholipids in vitro. J Virol 89:5714–5723. https://doi.org/10.1128/JVI.03711-14.
28. Pogany J, Nagy PD. 2012. p33-independent activation of a truncated p92 RNA-dependent RNA polymerase of tomato bushy stunt virus in yeast cell-free extract. J Virol 86:12025–12038. https://doi.org/10.1128/JVI.01303-12.
29. Feng Z, Xu K, Kovalev N, Nagy PD. 2019. Recruitment of Vps34 PI3K and enrichment of PI3P phosphoinositide in the viral replication compartment is crucial for replication of a positive-strand RNA virus. PLoS Pathog 15:e1007530. https://doi.org/10.1371/journal.ppat.1007530.
30. Xu K, Nagy PD. 2015. RNA virus replication depends on enrichment of phosphatidylethanolamine at replication sites in subcellular membranes. Proc Natl Acad Sci U S A 112:E1782–E1791. https://doi.org/10.1073/pnas.1418971112.
31. Nawaz-Ul-Rehman MS, Prasanth KR, Xu K, Sasvari Z, Kovalev N, de Castro Martín IF, Barajas D, Risco C, Nagy PD. 2016. Viral replication protein inhibits cellular cofilin actin depolymerization factor to regulate the actin network and promote viral replicase assembly. PLoS Pathog 12:e1005440. https://doi.org/10.1371/journal.ppat.1005440.
32. Panavas T, Hawkins CM, Panaviene Z, Nagy PD. 2005. The role of the p33:p33/p92 interaction domain in RNA replication and intracellular localization of p33 and p92 proteins of Cucumber necrosis tombusvirus. Virology 338:81–95. https://doi.org/10.1016/j.virol.2005.04.025.
33. Prasanth KR, Chuang C, Nagy PD. 2017. Co-opting ATP-generating glycolytic enzyme PGK1 phosphoglycerate kinase facilitates the assembly of viral replicase complexes. PLoS Pathog 13:e1006689. https://doi.org/10.1371/journal.ppat.1006689.
34. Chuang C, Prasanth KR, Nagy PD. 2017. The glycolytic pyruvate kinase is recruited directly into the viral replicase complex to generate ATP for RNA synthesis. Cell Host Microbe 22:639–652. https://doi.org/10.1016/j.chom.2017.10.004.
35. Inaba JI, Xu K, Kovalev N, Ramanathan H, Roy CR, Lindenbach BD, Nagy PD. 2019. Screening Legionella effectors for antiviral effects reveals Rab1 GTPase as a proviral factor coopted for tombusvirus replication.

Proc Natl Acad Sci U S A 116:21739–21747. https://doi.org/10.1073/pnas.1911108116.
36. Lin W, Liu Y, Molho M, Zhang S, Wang L, Xie L, Nagy PD. 2019. Co-opting the fermentation pathway for tombusvirus replication: compartmentalization of cellular metabolic pathways for rapid ATP generation. PLoS Pathog 15:e1008092. https://doi.org/10.1371/journal.ppat.1008092.
37. Nagy PD, Strating JR, van Kuppeveld FJ. 2016. Building viral replication organelles: close encounters of the membrane types. PLoS Pathog 12:e1005912. https://doi.org/10.1371/journal.ppat.1005912.
38. Sasvari Z, Kovalev N, Gonzalez PA, Xu K, Nagy PD. 2018. Assembly-hub function of ER-localized SNARE proteins in biogenesis of tombusvirus replication compartment. PLoS Pathog 14:e1007028. https://doi.org/10.1371/journal.ppat.1007028.
39. Barajas D, Xu K, de Castro Martin IF, Sasvari Z, Brandizzi F, Risco C, Nagy PD. 2014. Co-opted oxysterol-binding ORP and VAP proteins channel sterols to RNA virus replication sites via membrane contact sites. PLoS Pathog 10:e1004388. https://doi.org/10.1371/journal.ppat.1004388.
40. Panavas T, Serviene E, Brasher J, Nagy PD. 2005. Yeast genome-wide screen reveals dissimilar sets of host genes affecting replication of RNA viruses. Proc Natl Acad Sci U S A 102:7326–7331. https://doi.org/10.1073/pnas.0502604102.
41. Hsu F, Mao Y. 2015. The structure of phosphoinositide phosphatases: insights into substrate specificity and catalysis. Biochim Biophys Acta 1851:698–710. https://doi.org/10.1016/j.bbalip.2014.09.015.
42. Mesmin B, Bigay J, Moser von Filseck J, Lacas-Gervais S, Drin G, Antonny B. 2013. A four-step cycle driven by PI(4)P hydrolysis directs sterol/PI(4)P exchange by the ER-Golgi tether OSBP. Cell 155:830–843. https://doi.org/10.1016/j.cell.2013.09.056.
43. Stefan CJ, Manford AG, Baird D, Yamada-Hanff J, Mao Y, Emr SD. 2011. Osh proteins regulate phosphoinositide metabolism at ER-plasma membrane contact sites. Cell 144:389–401. https://doi.org/10.1016/j.cell.2010.12.034.
44. Zewe JP, Wills RC, Sangappa S, Goulden BD, Hammond GR. 2018. SAC1 degrades its lipid substrate PtdIns4P in the endoplasmic reticulum to maintain a steep chemical gradient with donor membranes. Elife 7:e35588. https://doi.org/10.7554/eLife.35588.
45. Del Bel LM, Brill JA. 2018. Sac1, a lipid phosphatase at the interface of vesicular and non-vesicular transport. Traffic 19:301–318. https://doi.org/10.1111/tra.12554.
46. Antonny B, Bigay J, Mesmin B. 2018. The oxysterol-binding protein cycle: burning off PI(4)P to transport cholesterol. Annu Rev Biochem 87:809–837. https://doi.org/10.1146/annurev-biochem-061516-044924.
47. Jackson CL, Walch L, Verbavatz JM. 2016. Lipids and their trafficking: an integral part of cellular organization. Dev Cell 39:139–153. https://doi.org/10.1016/j.devcel.2016.09.030.
48. Henne WM. 2016. Organelle remodeling at membrane contact sites. J Struct Biol 196:15–19. https://doi.org/10.1016/j.jsb.2016.05.003.
49. Raiborg C, Wenzel EM, Pedersen NM, Stenmark H. 2016. Phosphoinositides in membrane contact sites. Biochem Soc Trans 44:425–430. https://doi.org/10.1042/BST20150190.
50. Mesmin B, Antonny B. 2016. The counterflow transport of sterols and PI4P. Biochim Biophys Acta 1861:940–951. https://doi.org/10.1016/j.bbalip.2016.02.024.
51. Olkkonen VM, Li S. 2013. Oxysterol-binding proteins: sterol and phosphoinositide sensors coordinating transport, signaling and metabolism. Prog Lipid Res 52:529–538. https://doi.org/10.1016/j.plipres.2013.06.004.
52. Chung J, Torta F, Masai K, Lucast L, Czapla H, Tanner LB, Narayanaswamy P, Wenk MR, Nakatsu F, De Camilli P. 2015. Intracellular transport. PI4P/phosphatidylserine countertransport at ORP5- and ORP8-mediated ER-plasma membrane contacts. Science 349:428–432. https://doi.org/10.1126/science.aab1370.
53. Balla T. 2013. Phosphoinositides: tiny lipids with giant impact on cell regulation. Physiol Rev 93:1019–1137. https://doi.org/10.1152/physrev.00028.2012.
54. Piao H, Mayinger P. 2012. Growth and metabolic control of lipid signalling at the Golgi. Biochem Soc Trans 40:205–209. https://doi.org/10.1042/BST20110637.
55. Ijuin T, Takeuchi Y, Shimono Y, Fukumoto M, Tokuda E, Takenawa T. 2016. Regulation of CD44 expression and focal adhesion by Golgi phosphatidylinositol 4-phosphate in breast cancer. Cancer Sci 107:981–990. https://doi.org/10.1111/cas.12968.
56. Sohn M, Ivanova P, Brown HA, Toth DJ, Varnai P, Kim YJ, Balla T. 2016. Lenz-Majewski mutations in PTDSS1 affect phosphatidylinositol 4-phosphate metabolism at ER-PM and ER-Golgi junctions. Proc Natl Acad Sci U S A 113:4314–4319. https://doi.org/10.1073/pnas.1525719113.
57. Tokuda E, Itoh T, Hasegawa J, Ijuin T, Takeuchi Y, Irino Y, Fukumoto M, Takenawa T. 2014. Phosphatidylinositol 4-phosphate in the Golgi apparatus regulates cell-cell adhesion and invasive cell migration in human breast cancer. Cancer Res 74:3054–3066. https://doi.org/10.1158/0008-5472.CAN-13-2441.
58. Zhong R, Ye ZH. 2003. The SAC domain-containing protein gene family in Arabidopsis. Plant Physiol 132:544–555. https://doi.org/10.1104/pp.103.021444.
59. Despres B, Bouissonnie F, Wu HJ, Gomord V, Guilleminot J, Grellet F, Berger F, Delseny M, Devic M. 2003. Three SAC1-like genes show overlapping patterns of expression in Arabidopsis but are remarkably silent during embryo development. Plant J 34:293–306. https://doi.org/10.1046/j.1365-313x.2003.01720.x.
60. Zhong R, Burk DH, Nairn CJ, Wood-Jones A, Morrison WH, Ye Z-H. 2005. Mutation of SAC1, an Arabidopsis SAC domain phosphoinositide phosphatase, causes alterations in cell morphogenesis, cell wall synthesis, and actin organization. Plant Cell 17:1449–1466. https://doi.org/10.1105/tpc.105.031377.
61. Panavas T, Nagy PD. 2003. Yeast as a model host to study replication and recombination of defective interfering RNA of Tomato bushy stunt virus. Virology 314:315–325. https://doi.org/10.1016/s0042-6822(03)00436-7.
62. Thole JM, Vermeer JE, Zhang Y, Gadella TW, Jr, Nielsen E. 2008. Root hair defective 4 encodes a phosphatidylinositol-4-phosphate phosphatase required for proper root hair development in Arabidopsis thaliana. Plant Cell 20:381–395. https://doi.org/10.1105/tpc.107.054304.
63. Pogany J, Stork J, Li Z, Nagy PD. 2008. In vitro assembly of the Tomato bushy stunt virus replicase requires the host Heat shock protein 70. Proc Natl Acad Sci U S A 105:19956–19961. https://doi.org/10.1073/pnas.0810851105.
64. Kovalev N, Pogany J, Nagy PD. 2014. Template role of double-stranded RNA in tombusvirus replication. J Virol 88:5638–5651. https://doi.org/10.1128/JVI.03842-13.
65. Mendu V, Chiu M, Barajas D, Li Z, Nagy PD. 2010. Cpr1 cyclophilin and Ess1 parvulin prolyl isomerases interact with the tombusvirus replication protein and inhibit viral replication in yeast model host. Virology 406:342–351. https://doi.org/10.1016/j.virol.2010.07.022.
66. Wu CY, Nagy PD. 2019. Blocking tombusvirus replication through the antiviral functions of DDX17-like RH30 DEAD-box helicase. PLoS Pathog 15:e1007771. https://doi.org/10.1371/journal.ppat.1007771.
67. Xu K, Huang TS, Nagy PD. 2012. Authentic in vitro replication of two tombusviruses in isolated mitochondrial and endoplasmic reticulum membranes. J Virol 86:12779–12794. https://doi.org/10.1128/JVI.00973-12.
68. Richardson LG, Clendening EA, Sheen H, Gidda SK, White KA, Mullen RT. 2014. A unique N-terminal sequence in the Carnation Italian ringspot virus p36 replicase-associated protein interacts with the host cell ESCRT-I component Vps23. J Virol 88:6329–6344. https://doi.org/10.1128/JVI.03840-13.
69. Manford AG, Stefan CJ, Yuan HL, Macgurn JA, Emr SD. 2012. ER-to-plasma membrane tethering proteins regulate cell signaling and ER morphology. Dev Cell 23:1129–1140. https://doi.org/10.1016/j.devcel.2012.11.004.
70. Cai Y, Deng Y, Horenkamp F, Reinisch KM, Burd CG. 2014. Sac1-Vps74 structure reveals a mechanism to terminate phosphoinositide signaling in the Golgi apparatus. J Cell Biol 206:485–491. https://doi.org/10.1083/jcb.201404041.
71. Audhya A, Foti M, Emr SD. 2000. Distinct roles for the yeast phosphatidylinositol 4-kinases, Stt4p and Pik1p, in secretion, cell growth, and organelle membrane dynamics. Mol Biol Cell 11:2673–2689. https://doi.org/10.1091/mbc.11.8.2673.
72. Villasuso AL, Racagni GE, Machado EE. 2008. Phosphatidylinositol kinases as regulators of GA-stimulated alpha-amylase secretion in barley (Hordeum vulgare). Physiol Plant 133:157–166. https://doi.org/10.1111/j.1399-3054.2008.01050.x.
73. Krinke O, Ruelland E, Valentova O, Vergnolle C, Renou JP, Taconnat L, Flemr M, Burketova L, Zachowski A. 2007. Phosphatidylinositol 4-kinase activation is an early response to salicylic acid in Arabidopsis suspension cells. Plant Physiol 144:1347–1359. https://doi.org/10.1104/pp.107.100842.
74. Birkeland HC, Stenmark H. 2004. Protein targeting to endosomes and phagosomes via FYVE and PX domains. Curr Top Microbiol Immunol 282:89–115. https://doi.org/10.1007/978-3-642-18805-3_4.
75. Del Campo CM, Mishra AK, Wang YH, Roy CR, Janmey PA, Lambright

DG. 2014. Structural basis for PI(4)P-specific membrane recruitment of the Legionella pneumophila effector DrrA/SidM. Structure 22:397–408. https://doi.org/10.1016/j.str.2013.12.018.
76. Sasvari Z, Gonzalez PA, Rachubinski RA, Nagy PD. 2013. Tombusvirus replication depends on Sec39p endoplasmic reticulum-associated transport protein. Virology 447:21–31. https://doi.org/10.1016/j.virol.2013.07.039.
77. Imura Y, Molho M, Chuang C, Nagy PD. 2015. Cellular Ubc2/Rad6 E2 ubiquitin-conjugating enzyme facilitates tombusvirus replication in yeast and plants. Virology 484:265–275. https://doi.org/10.1016/j.virol.2015.05.022.
78. Barajas D, Martin IF, Pogany J, Risco C, Nagy PD. 2014. Noncanonical role for the host Vps4 AAA+ ATPase ESCRT protein in the formation of tomato bushy stunt virus replicase. PLoS Pathog 10:e1004087. https://doi.org/10.1371/journal.ppat.1004087.
79. Li Z, Barajas D, Panavas T, Herbst DA, Nagy PD. 2008. Cdc34p ubiquitin-conjugating enzyme is a component of the tombusvirus replicase complex and ubiquitinates p33 replication protein. J Virol 82:6911–6926. https://doi.org/10.1128/JVI.00702-08.
80. Prasanth KR, Barajas D, Nagy PD. 2015. The proteasomal Rpn11 metalloprotease suppresses tombusvirus RNA recombination and promotes viral replication via facilitating assembly of the viral replicase complex. J Virol 89:2750–2763. https://doi.org/10.1128/JVI.02620-14.
81. Chuang C, Prasanth KR, Nagy PD. 2015. Coordinated function of cellular DEAD-box helicases in suppression of viral RNA recombination and maintenance of viral genome integrity. PLoS Pathog 11:e1004680. https://doi.org/10.1371/journal.ppat.1004680.
82. Kovalev N, Pogany J, Nagy PD. 2012. A co-opted DEAD-box RNA helicase enhances tombusvirus plus-strand synthesis. PLoS Pathog 8:e1002537. https://doi.org/10.1371/journal.ppat.1002537.
83. Pogany J, White KA, Nagy PD. 2005. Specific binding of tombusvirus replication protein p33 to an internal replication element in the viral RNA is essential for replication. J Virol 79:4859–4869. https://doi.org/10.1128/JVI.79.8.4859-4869.2005.
84. Kovalev N, Inaba JI, Li Z, Nagy PD. 2017. The role of co-opted ESCRT proteins and lipid factors in protection of tombusviral double-stranded RNA replication intermediate against reconstituted RNAi in yeast. PLoS Pathog 13:e1006520. https://doi.org/10.1371/journal.ppat.1006520.
85. Altan-Bonnet N, Balla T. 2012. Phosphatidylinositol 4-kinases: hostages harnessed to build panviral replication platforms. Trends Biochem Sci 37:293–302. https://doi.org/10.1016/j.tibs.2012.03.004.
86. Li Z, Pogany J, Tupman S, Esposito AM, Kinzy TG, Nagy PD. 2010. Translation elongation factor 1A facilitates the assembly of the tombusvirus replicase and stimulates minus-strand synthesis. PLoS Pathog 6:e1001175. https://doi.org/10.1371/journal.ppat.1001175.
87. Jonczyk M, Pathak KB, Sharma M, Nagy PD. 2007. Exploiting alternative subcellular location for replication: tombusvirus replication switches to the endoplasmic reticulum in the absence of peroxisomes. Virology 362:320–330. https://doi.org/10.1016/j.virol.2007.01.004.
88. den Boon JA, Diaz A, Ahlquist P. 2010. Cytoplasmic viral replication complexes. Cell Host Microbe 8:77–85. https://doi.org/10.1016/j.chom.2010.06.010.
89. Randall G, Panis M, Cooper JD, Tellinghuisen TL, Sukhodolets KE, Pfeffer S, Landthaler M, Landgraf P, Kan S, Lindenbach BD, Chien M, Weir DB, Russo JJ, Ju J, Brownstein MJ, Sheridan R, Sander C, Zavolan M, Tuschl T, Rice CM. 2007. Cellular cofactors affecting hepatitis C virus infection and replication. Proc Natl Acad Sci U S A 104:12884–12889. https://doi.org/10.1073/pnas.0704894104.
90. Oh HS, Banerjee S, Aponte-Diaz D, Sharma SD, Aligo J, Lodeiro MF, Ning G, Sharma R, Arnold JJ, Cameron CE. 2018. Multiple poliovirus-induced organelles suggested by comparison of spatiotemporal dynamics of membranous structures and phosphoinositides. PLoS Pathog 14:e1007036. https://doi.org/10.1371/journal.ppat.1007036.
91. Reiss S, Rebhan I, Backes P, Romero-Brey I, Erfle H, Matula P, Kaderali L, Poenisch M, Blankenburg H, Hiet MS, Longerich T, Diehl S, Ramirez F, Balla T, Rohr K, Kaul A, Buhler S, Pepperkok R, Lengauer T, Albrecht M, Eils R, Schirmacher P, Lohmann V, Bartenschlager R. 2011. Recruitment and activation of a lipid kinase by hepatitis C virus NS5A is essential for integrity of the membranous replication compartment. Cell Host Microbe 9:32–45. https://doi.org/10.1016/j.chom.2010.12.002.
92. Shengjuler D, Chan YM, Sun S, Moustafa IM, Li ZL, Gohara DW, Buck M, Cremer PS, Boehr DD, Cameron CE. 2017. The RNA-binding site of poliovirus 3C protein doubles as a phosphoinositide-binding domain. Structure 25:1875–1886. https://doi.org/10.1016/j.str.2017.11.001.
93. Dorobantu CM, Albulescu L, Harak C, Feng Q, van Kampen M, Strating JR, Gorbalenya AE, Lohmann V, van der Schaar HM, van Kuppeveld FJ. 2015. Modulation of the host lipid landscape to promote RNA virus replication: the picornavirus encephalomyocarditis virus converges on the pathway used by hepatitis C virus. PLoS Pathog 11:e1005185. https://doi.org/10.1371/journal.ppat.1005185.
94. Roulin PS, Lotzerich M, Torta F, Tanner LB, van Kuppeveld FJ, Wenk MR, Greber UF. 2014. Rhinovirus uses a phosphatidylinositol 4-phosphate/cholesterol counter-current for the formation of replication compartments at the ER-Golgi interface. Cell Host Microbe 16:677–690. https://doi.org/10.1016/j.chom.2014.10.003.
95. Ishikawa-Sasaki K, Nagashima S, Taniguchi K, Sasaki J. 2018. A model of OSBP-mediated cholesterol supply to Aichi virus RNA replication sites involving protein-protein interactions among viral proteins, ACBD3, OSBP, VAP-A/B, and SAC1. J Virol 92:e01952-17. https://doi.org/10.1128/JVI.01952-17.
96. Berger KL, Kelly SM, Jordan TX, Tartell MA, Randall G. 2011. Hepatitis C virus stimulates the phosphatidylinositol 4-kinase III alpha-dependent phosphatidylinositol 4-phosphate production that is essential for its replication. J Virol 85:8870–8883. https://doi.org/10.1128/JVI.00059-11.
97. Bishe B, Syed G, Siddiqui A. 2012. Phosphoinositides in the hepatitis C virus life cycle. Viruses 4:2340–2358. https://doi.org/10.3390/v4102340.
98. Harak C, Radujkovic D, Taveneau C, Reiss S, Klein R, Bressanelli S, Lohmann V. 2014. Mapping of functional domains of the lipid kinase phosphatidylinositol 4-kinase type III alpha involved in enzymatic activity and hepatitis C virus replication. J Virol 88:9909–9926. https://doi.org/10.1128/JVI.01063-14.
99. Derre I. 2017. Hijacking of membrane contact sites by intracellular bacterial pathogens. Adv Exp Med Biol 997:211–223. https://doi.org/10.1007/978-981-10-4567-7_16.
100. Mnaimneh S, Davierwala AP, Haynes J, Moffat J, Peng WT, Zhang W, Yang X, Pootoolal J, Chua G, Lopez A, Trochesset M, Morse D, Krogan NJ, Hiley SL, Li Z, Morris Q, Grigull J, Mitsakakis N, Roberts CJ, Greenblatt JF, Boone C, Kaiser CA, Andrews BJ, Hughes TR. 2004. Exploration of essential gene functions via titratable promoter alleles. Cell 118:31–44. https://doi.org/10.1016/j.cell.2004.06.013.
101. Janke C, Magiera MM, Rathfelder N, Taxis C, Reber S, Maekawa H, Moreno-Borchart A, Doenges G, Schwob E, Schiebel E, Knop M. 2004. A versatile toolbox for PCR-based tagging of yeast genes: new fluorescent proteins, more markers and promoter substitution cassettes. Yeast 21:947–962. https://doi.org/10.1002/yea.1142.
102. Barajas D, Li Z, Nagy PD. 2009. The Nedd4-type Rsp5p ubiquitin ligase inhibits tombusvirus replication by regulating degradation of the p92 replication protein and decreasing the activity of the tombusvirus replicase. J Virol 83:11751–11764. https://doi.org/10.1128/JVI.00789-09.
103. Panaviene Z, Panavas T, Serva S, Nagy PD. 2004. Purification of the cucumber necrosis virus replicase from yeast cells: role of coexpressed viral RNA in stimulation of replicase activity. J Virol 78:8254–8263. https://doi.org/10.1128/JVI.78.15.8254-8263.2004.
104. Yoo SD, Cho YH, Sheen J. 2007. Arabidopsis mesophyll protoplasts: a versatile cell system for transient gene expression analysis. Nat Protoc 2:1565–1572. https://doi.org/10.1038/nprot.2007.199.
105. Jaag HM, Nagy PD. 2009. Silencing of Nicotiana benthamiana Xrn4p exoribonuclease promotes tombusvirus RNA accumulation and recombination. Virology 386:344–352. https://doi.org/10.1016/j.virol.2009.01.015.
106. Rajendran KS, Pogany J, Nagy PD. 2002. Comparison of turnip crinkle virus RNA-dependent RNA polymerase preparations expressed in Escherichia coli or derived from infected plants. J Virol 76:1707–1717. https://doi.org/10.1128/jvi.76.4.1707-1717.2002.
107. Pogany J, Nagy PD. 2008. Authentic replication and recombination of Tomato bushy stunt virus RNA in a cell-free extract from yeast. J Virol 82:5967–5980. https://doi.org/10.1128/JVI.02737-07.
108. Kovalev N, Nagy PD. 2013. Cyclophilin A binds to the viral RNA and replication proteins, resulting in inhibition of tombusviral replicase assembly. J Virol 87:13330–13342. https://doi.org/10.1128/JVI.02101-13.